Winter 2018

Robocatch: Design and Making of a Hand-Held Spillage-Free Specimen Retrieval Robot for Laparoscopic Surgery

Farid Tavakkolmoghaddam
Old Dominion University

ROBOCATCH: DESIGN AND MAKING OF A HAND-HELD SPILLAGE-FREE SPECIMEN RETRIEVAL ROBOT FOR LAPAROSCOPIC SURGERY

by

Farid Tavakkolmoghaddam
B.S. September 2015, Islamic Azad University, Iran

A Thesis Submitted to the Faculty of
Old Dominion University in Partial Fulfillment of the
Requirements for the Degree of

MASTER OF SCIENCE

MECHANICAL ENGINEERING

OLD DOMINION UNIVERSITY
December 2018

Approved by:

Krishnanand Kaipa (Director)

Stacie Ringleb (Member)

Michel Audette (Member)

ABSTRACT

ROBOCATCH: DESIGN AND MAKING OF A HAND-HELD SPILLAGE-FREE SPECIMEN RETRIEVAL ROBOT FOR LAPAROSCOPIC SURGERY

Farid Tavakkolmoghaddam

Old Dominion University, 2018

Director: Krishnanand Kaipa

Specimen retrieval is an important step in laparoscopy, a minimally invasive surgical procedure performed to diagnose and treat a myriad of medical pathologies in fields ranging from gynecology to oncology. Specimen retrieval bags (SRBs) are used to facilitate this task, while minimizing contamination of neighboring tissues and port-sites in the abdominal cavity. This manual surgical procedure requires usage of multiple ports, creating a traffic of simultaneous operations of multiple instruments in a limited shared workspace. The skill-demanding nature of this procedure makes it time-consuming, leading to surgeons' fatigue and operational inefficiency. This thesis presents the design and making of RoboCatch, a novel hand-held robot that aids a surgeon in performing spillage-free retrieval of operative specimens in laparoscopic surgery. The proposed design significantly modifies and extends conventional instruments that are currently used by surgeons for the retrieval task: The core instrumentation of RoboCatch comprises a webbed three-fingered grasper and atraumatic forceps that are concentrically situated in a folded configuration inside a trocar. The specimen retrieval task is achieved in six stages: 1) The trocar is introduced into the surgical site through an instrument port, 2) the three webbed fingers slide out of the tube and simultaneously unfold in an umbrella like-fashion, 3) the forceps slide toward, and grasp, the excised specimen, 4) the forceps retract the grasped specimen into the center of the surrounding grasper, 5) the grasper closes to achieve a secured containment of the specimen, and

6) the grasper, along with the contained specimen, is manually removed from the abdominal cavity. The resulting reduction in the number of active ports reduces obstruction of the port-site and increases the procedure's efficiency. The design process was initiated by acquiring crucial parameters from surgeons and creating a design table, which informed the CAD modeling of the robot structure and selection of actuation units and fabrication material. The robot prototype was first examined in CAD simulation and then fabricated using an Objet30 Prime 3D printer. Physical validation experiments were conducted to verify the functionality of different mechanisms of the robot. Further, specimen retrieval experiments were conducted with porcine meat samples to test the feasibility of the proposed design. Experimental results revealed that the robot was capable of retrieving masses of specimen ranging from 1 gram to 50 grams. The making of RoboCatch represents a significant step toward advancing the frontiers of hand-held robots for performing specimen retrieval tasks in minimally invasive surgery.

This thesis is dedicated to my family, my mother, my father, and my sister.

ACKNOWLEDGMENTS

I would like to thank my advisor, Dr. Krishnanand Kaipa for guiding and supporting me over this whole process. You have set an example of excellence as a researcher, mentor, instructor, and role model. I would like to thank Dr. Sebastian Bawab, the Chair of the MAE Department, for his constant support of my research. I wish to thank the members of my dissertation committee: Dr. Stacie Ringleb and Dr. Michel Audette for generously offering their time, support, guidance, and good will throughout the preparation and review of this document.

I would like to thank my fellow labmates, Siqin Dong and Parimal Prajapati, who have contributed to this research. I would like to thank all other CRAM lab members Michael Wang, Nicole Tennant, and Manali Bhadugale. Special thanks goes to my friend Ramin Rabiee for helping me with thesis formatting and supporting me throughout my stay here. Thanks also to Ali Parva, Maryam Ehsaei, Elham Sharifi, Mohammad Mahdavi, Soheil Sohrabi, and Arash Niroomandi. I am very grateful to all of you. You have always given me energy to keep on going and encouraged me throughout this process.

I would especially like to thank my amazing family for the love, support, and constant encouragement I have gotten over the years. In particular, I would like to thank my parents, my sister, and my aunt Salma. You never stopped believing in me even when I did not believe in myself. I undoubtedly could not have done this without you and I am forever grateful for that.

TABLE OF CONTENTS

Page

LIST OF TABLES

Table Page

LIST OF FIGURES

CHAPTER 1

1 INTRODUCTION

1.1 Motivation

1.1.1 SPECIMEN RETRIEVAL TASKS IN LAPAROSCOPIC SURGERY

Specimen retrieval is an important step in laparoscopy, a minimally invasive surgical procedure performed to diagnose and treat a myriad of medical pathologies in fields ranging from gynecology (e.g., removal of adnexal cysts, myoma, myomatous uteri, etc.) to oncology (e.g., removal of tumors in liver [1] and esophageal [2] cancers). The retrieval task typically involves extraction of a resected/excised specimen, residing in the abdominal cavity, completely outside of the patient's body. One of the primary challenges in this context is spillage of the content being retrieved, which may cause dissemination of disease, infection, or malignancy. This issue is addressed to a large extent by specimen retrieval bags (SRBs), which have long been used in minimally invasive surgery for contained removal of tissues, organs, and bones from the body cavity. SRBs facilitate the extraction of the operative specimen from the body cavity, while minimizing the risks of contamination of the neighboring tissue, organs, and wound tract [3].

Although considered as crucial tools for removal of operative specimens in laparoscopy, SRBs present a number of challenges:

1) An immense laparoscopic skill is required to entrap and safely extract laparoscopic specimens [4]. This manual surgical procedure requires usage of multiple ports, creating a traffic of simultaneous operations of multiple instruments in a limited shared workspace. The skill-demanding nature of the retrieval procedure using SRBs is time-consuming (conventional specimen entrapment takes up to 10 minutes on average) and could lead to surgeons' fatigue and operational inefficiency.

2) Some SRBs have a continuously open mouth that could allow the contained specimens to slip or fall out [5]. This issue is addressed to some extent by other types of SRBs that have a purse-string closure mechanism. However, the bag-closing is permanent, thereby disallowing further placement of other specimens after closure is achieved.
3) The number of required instruments for the successful specimen removal procedure depends on the opening mechanism of the specimen bag. Whereas a *manually opening bag* (e.g., Endo Bag™ by Medtronic Inc.) uses two graspers to unfold the bag and keep it in position, and a third grasper to retract the excised tissue and place it inside the bag, an a*utomatically opening bag* (Endo Catch™ by Medtronic Inc.) gets delivered to the abdomen via a slender shaft and opens automatically when the inner shaft is pushed forward. This requires fewer graspers, but generally the latter is more expensive than the former.

In conventional multiport laparoscopic surgery (MLS), for a specimen to be removed from the abdominal cavity, four or more ports are occupied at the same time to retract the excised specimen and securely place it inside the bag. This task becomes challenging since the articulation of rigid instruments within the limited confinements of the abdominal cavity in laparoscopic surgeries is an exacting task and a critical determinant of surgical performance [6]. In single port or "single Incision" laparoscopic surgery (SIL), specimen removal is even more challenging, given that all instruments are operated within the same port. As a result, instrument triangulation, coupled with linear vision and lack of external workspace, make the specimen retrieval a laborious and time-consuming task for both MLS and SIL surgeries.

1.1.2 ROBOT-ASSISTED SPECIMEN RETRIEVAL

Recent advances in surgical robotics, a sub-field in medical robotics, attempt to overcome some of the limitations of manual laparoscopic procedures by augmenting the surgeons' capabilities while performing suturing, incision, and retrieval tasks [7]. A multitude of technologies in the general field of robotic grasping and manipulation can be applied to robotic surgery. However, task requirements specific to laparoscopy have resulted in highly specialized robotic designs, which can be classified into master-slave tele-operated robots [8], cooperatively controlled robots [9, 10], and hand-held robots [11]. Progress of master-slave and cooperatively-controlled robots in clinical applications has been impressive and noteworthy. However, drawbacks like high system costs, large footprint in the operation theaters, and extensive learning curves for acquiring the necessary operation skills prohibit more wide-spread use of these systems. Hand-held robots address these limitations by leveraging the complementary strengths of the surgeon (e.g., years of practiced surgical skills, dexterity, and compliance) and the robot (e.g., compactness, accuracy, repeatability, etc). The compactness of hand-held robots enables their seamless integration with the normal workflow of the operation rooms with little or no setup time [11]. In addition, hand-held devices cost significantly less due to reduced actuation DoF, sensors, and control units. The focus in this thesis is on robotic approaches for specimen retrieval tasks using hand-held robots.

1.2 Thesis Goals and Contributions

This thesis presents the design of a novel hand-held laparoscopic specimen retrieval robot for spillage-free extraction of a variety of operative specimens in laparoscopic surgery. The proposed approach represents a significant step toward mitigating the drawbacks of the current specimen retrieval methods in laparoscopic surgery. Three principal research questions related to

the surgical robot's design are addressed: 1) How to integrate two different mechanisms of grasping and retrieval bag into one single device? 2) How to integrate electrical actuation into already existing mechanical systems? 3) How do we achieve a practical design, while using the minimum number of electrical actuators?

Answers to these questions are not straightforward. First, many task-specific considerations need to be addressed when designing a surgical robot geared toward a practical clinical application. Second, the design should not diverge from, rather closely adhere to, the core principles of MIS like minimal invasiveness, ease of operation, ergonomics, and low operation costs. Third, the robot should minimize control complexities. Finally, the robot's design must account for factors such as safety, sterilizability, minimum DoF for the robot's motion, and accuracy. The anticipated outcome of the proposed design is an improved instrument triangulation and a reduction in surgeon's workload during task execution. This thereby could contribute to enhancing the surgeon's focus on the task, rather than being concerned with simultaneous articulation of too many instruments in a limited internal and external workspace.

The proposed design significantly differs from other conventional devices: The innovative design reduces the number of active ports required for removal of specimens by combining two laparoscopic instruments—a specimen retrieval bag actuated by a three-fingered grasper and an atraumatic grasping forceps—concentrically housed within the device. During the insertion through the abdominal wall, the device first grasps the resected specimen and then brings it to the center of the specimen bag. The specimen is then engulfed by the fingers that are attached to the specimen bag and then removed from the abdomen, leading to a spillage-free retrieval of the resected specimen. Moreover, the resulting reduction in the number of ports reduces obstruction of the port-site and increases the procedure's efficiency.

The design process was initiated by acquiring crucial parameters from the surgeons and creating a design table, which guided the CAD modeling of the robot structure and selection of actuation units and the fabrication material. The various mechanisms of the robot were first carefully examined in the CAD simulation environment and then the prototype was fabricated using an Objet30 Prime 3D printer. A commercially available atraumatic grasper was modified and integrated into the device. Physical validation experiments were conducted to investigate the functionality of different mechanisms of the robot. Further, specimen retrieval experiments were conducted using porcine meat samples to test the feasibility of the proposed design. Experimental results revealed that the robot was capable of spillage-free retrieval of specimen of masses ranging from 1 gram to 50 grams.

CHAPTER 2

2 RELATED WORK

2.1 Minimally Invasive Surgery

Substantial improvements in the art and science of surgery were made over the last 150 years since the introduction of antiseptic techniques by Lister, including improved anesthetic agents, antibiotics, surgical nutrition, and organ transplantation, in which the basic tools remained unchanged [12]. The core surgical tasks—cutting and sewing—with hand instruments and direct visualization of, and contact with, the organ/tissue have remained the same. However, the last three decades has witnessed a change in surgical methods in a manner that involves minimizing the invasiveness of the surgery. *Minimally invasive surgery* (MIS)" (or *keyhole* surgery or minimal access surgery) is any type of surgical procedure that employs techniques to reduce the invasiveness of the surgery. In MIS, the need for having a direct physical contact between the surgeon's hand and the patient's organ/tissue is eliminated, since the surgeon operates the instruments from outside of patient's body through small ports that give access to the intended site of operation. The benefits to this approach, in comparison with open surgery, are less trauma to body tissues and organs, less bleeding, smaller incisions, smaller post-operative scars, faster recovery, and reduced intraoperative complications.

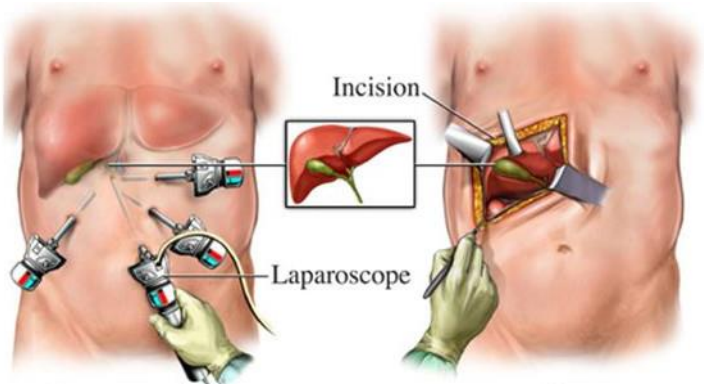

Fig. 1 MIS vs. open surgery [60]

Laparoscopic cholecystectomy, introduced in 1987, marked a beginning of an explosive growth in MIS [8]. Since then, advances in techniques and applications of MIS have been directly correlated with technological developments of instrumentation in the field. Although emergence of MIS is arguably the greatest innovation in surgery over the last thirty years [13], there exists some drawbacks. For example, three-dimensional images are projected on a two-dimensional screen, resulting in a loss of depth in the visualization of the surgical site. Factors like stability, focus, and tilt depend on the camera operator and an ability to follow the natural movement of the surgeon's eyes is limited [14]. Loss of wrist articulation, poor touch feedback, and poor ergonomics of the tools are some other limitations of MIS [15]. Additionally, the use of rigid instruments introduces fulcrum effect, a counter-intuitive movement at the instrument's tip, which is in an opposite direction to the surgeon's hand movement.

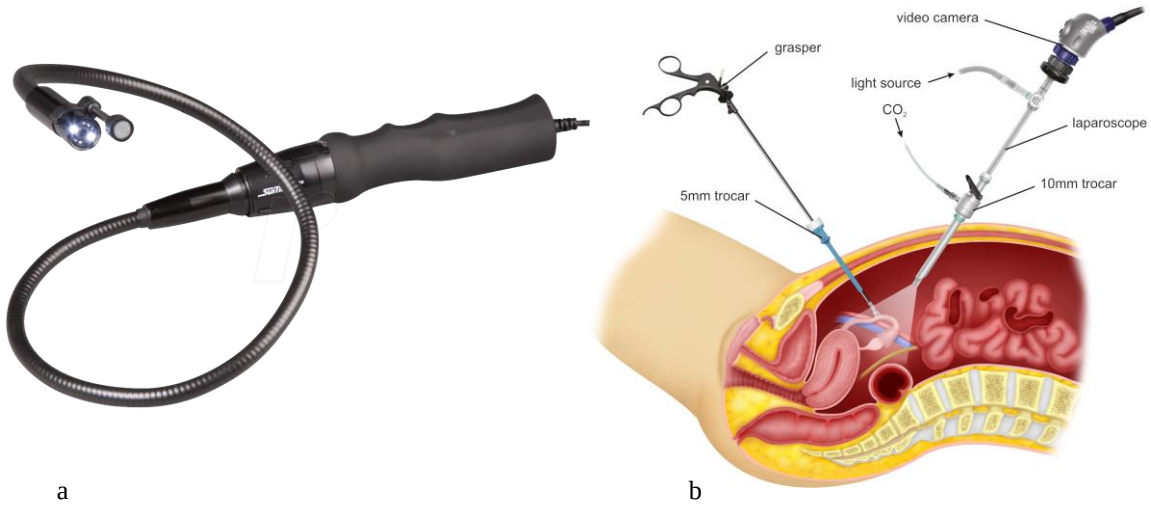

a b

Fig. 2 Conventional laparoscopic instruments [61, 62]

a) ENDO KAM Endoscope [61], b) Phantom view inside the abdomen in a laparoscopic procedure [62]. A laparoscope is use for the visualization of the surgical site. Instruments are passed through small incisions and manipulate the tissue inside the abdominal cavity.

In MIS, usually an endoscope and slender instruments are delivered inside the body cavity through small incisions. In multiport laparoscopic surgery (MLS), four or more small incisions are

made to deliver the instruments to the body cavity. Recently, there has been developments in single incision laparoscopic surgery (SIL), a less invasive approach that causes minimal trauma to the abdominal wall by using a single incision through the umbilical port for delivery of instruments to the body cavity. Key benefits of SIL over MLS are faster recovery and less cosmetic footprint after surgery. However, there are some underlying manipulation challenges in SIL that have hindered its widespread use in operation theaters. The size of the incision and the use of a single port with multiple accesses limit the possibility of navigation due to the reduced space in which the laparoscope and instruments have to operate [16]. Additionally, using a single port for accessing the abdomen makes instruments triangulation a challenge, since most tools that are used are rigid and have a limited maneuverability during operation in a limited space. This not only results in a limited manipulation of the tissue but also adds to the total operation time that could result in the surgeon's fatigue and loss of ergonomics. Natural orifice transluminal endoscopic surgery (NOTES), whereby scar-less operations can be performed by entering the body cavity through natural orifices, followed by an internal incision in the surgical site of interest, is another alternative approach to several laparoscopic operations such as gallbladder or cyst removal [17].

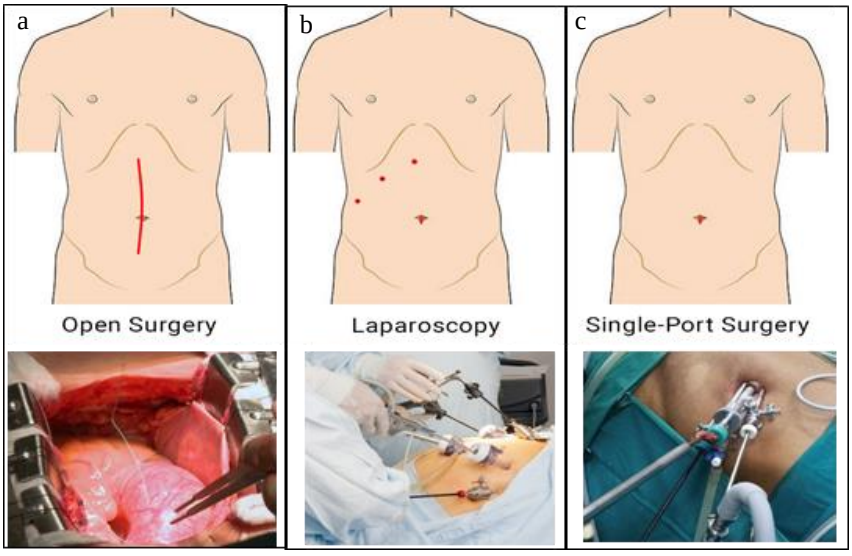

Fig. 3 Open surgery (a), multiport Laparoscopic surgery (b), single incision Laparoscopic surgery (c) [63- 66]

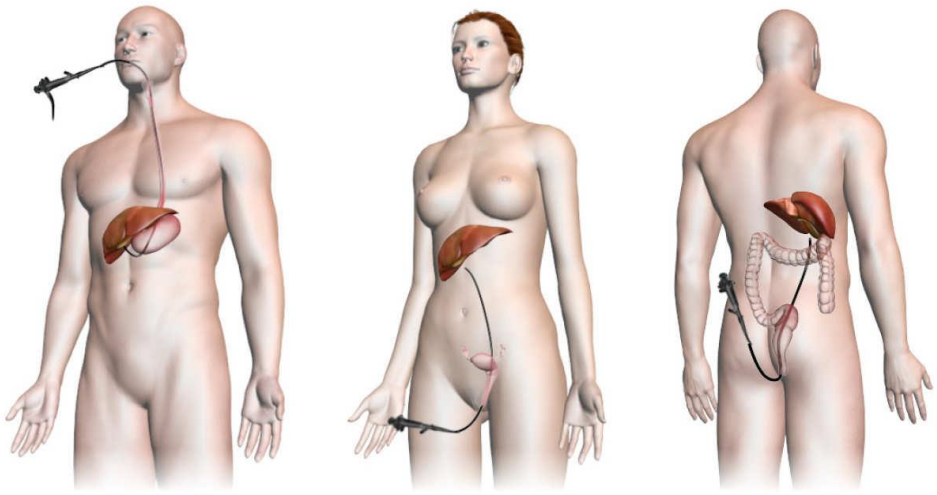

Fig. 4 Transgastric (left), transvaginal (middle) and transrectal (right) NOTES procedures [67]

2.2 Specimen Retrieval Tasks in MIS

Although MIS has solved many technical and physical challenges present in the open surgery, some challenges are still present. A persistent problem in operative laparoscopy is the exteriorization of intra-abdominal masses once they have been freed from the targeted tissue or organ from the abdominal cavity [18]. There are various options available for specimen retrieval including direct specimen retrieval, morcellation within an insufflated specimen retrieval bag, and retrieval by specimen retrieval bag [5]. Direct retrieval of specimens is used in cases where the excised tissue does not pose any risks in contaminating the abdominal cavity or the wound tract. Usually umbilical ports (in cases of multiport laparoscopic surgery) or the port for hand assistance (in cases of hand-assisted laparoscopy surgery) is used for the direct removal of the operative specimen. Electrical power morcellation is generally used in cases where excised specimens are large and removal of them with or without specimen bags pose difficulty and requires enlargement of the incision. In these scenarios, morcellator is employed to cut the tissue into smaller pieces and export the fragments outside of the surgical site. Morcellation can be done with or without specimen bags. However, since the risk of spillage of the cyst contents is associated with

complications such as pseudomyxoma peritonei (mucinous ystadenoma), chemical peritonitis (dermoid cyst) and the potential dissemination of malignancy [19], morcellation within an insufflated bag is suggested in cases where the risk of malignancy is suspected for the excised tissue.

2.3 Specimen Retrieval Bags

Specimen retrieval bags (SRBs) have long been used in minimally invasive surgery for contained removal of tissues, organs, and bones from the body cavity. They facilitate the extraction of the operative specimen from the body cavity while minimizing the risks of contamination of the neighboring tissue, organs, and wound tract [3].For instance, in cholecystectomy, specimen bags are used to collect gallbladder and occasionally spilled gallstones during the removal of gallbladder. Use of SRB helps minimizing the spillage of gallstones and bile that may cause various adverse post-operative issues such as infection, abscess, inflammation, fibrosis, adhesions, cutaneous sinuses, or generalized septicemia [20]. Another major use of specimen retrieval bags is in Gynecology surgery where specimen bags are used for removal of benign adnexal masses, ovarian dermoid cysts, tubal cysts, and fallopian tubes. In these cases, usage of SRB is preferred since the spillage of malignant cysts may risk an inadvertent cell seeding and infection of healthy neighboring tissues that may result in the upstaging of the disease [21]. In Urological surgery such as in prostatectomy, simple nephrectomy, and adrenalectomy, SRBs are used to enable extraction of larger and more friable specimens from the abdomen that are otherwise very challenging if not impossible to remove with conventional laparoscopic instruments. Table 1. represents some physical characteristics of specimens that are routinely removed with the help of SRBs in Gynecology surgery based on random examination of two groups of 25 individuals [22].

Table 1. The operative outcome of 50 patients receiving laparoscopic adnexal surgery

Item	Group 1	Group 2
Adnexal Cyst size (cm)	7.4±3.0	8.4±3.2
Cyst volume (ml)	204±338	241±262
Cyst weight (gr)	18.4±23.8	29.7±29.4
Cyst retrieval time (min)	0.7±1.8	4.9±12.6

*Data is expressed as mean±standard deviation. [48]

There are a variety of commercially available specimen retrieval bags, which have been designed for different specimen sizes and pathologies. An ideal specimen entrapment system should be easy to manipulate, with easy entrapment mechanism, good visibility, and the need for a minimal number of ports [5]. Although SRB is considered a crucial tool for the removal of operative specimens in laparoscopic surgery, however, use of it presents a number of challenges that are addressed in this thesis. One problem is that significant laparoscopic skill is required to entrap and safely extract laparoscopic specimens [4]. In addition, some bags have continuously open mouth that could allow the specimens put into it to slip or fall out [5]. On the other hand, some bags have thread that allows them to close off their opening after the specimen has been placed inside them. However, the problem with these types of bags is that closing of the bag is permeant and therefore, no other specimens can be placed inside them after they are sealed off. Conventional entrapment of specimens on average takes around 4-10 minutes to complete, which combined with its inherently skill demanding nature, could result in surgeon's fatigue and loss of accuracy. Moreover, the number of required instruments for the successful specimen removal procedure depends on the opening mechanism of the specimen bag.

Specimen retrieval bags are divided into two categories based on their opening mechanisms: "*manually opening bag*" and "*automatically opening bag*". Manually opening bags

have a manual opening mechanism, where usually two graspers are used to unfold the bag and keep the bag in position by holding the edges of the bag open while the third grasper retracts the excised tissue and places it inside the bag. An example of this type of specimen bag is Endo Bag™ manufactured by Medtronic Inc. *Automatically opening bag* is another type of specimen bag with an automatic opening mechanism where the bag is delivered to the abdomen via a slender shaft. The bag opens automatically when the inner shaft is pushed forward. This type of opening is easier to operate and requires fewer graspers to achieve the same goal but generally is more expensive in comparison with the manual opening bag. An Example of this type of specimen bags is Endo Catch™ manufactured by Medtronic Inc. Fig. 5 shows an example of a manually opening specimen bag (Endo Bag™, Medtronic Inc.), and an automatically opening bag (Endo Catch™, Medtronic Inc.)

Fig. 5 Types of specimen retrieval bags [68]

a) A manually opening specimen bag (Endo Bag™, Medtronic Inc.), and b) An automatically opening bag (Endo Catch™, Medtronic Inc.).

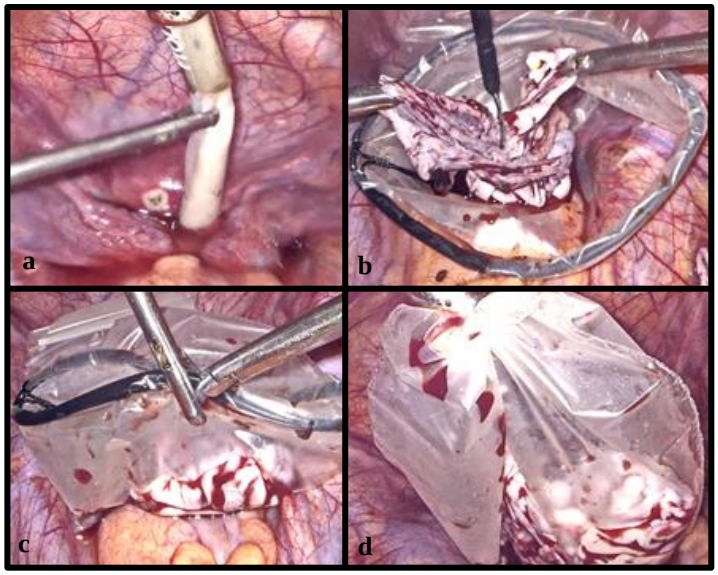

Fig. 6 Stages of specimen removal using a manually opening bag [69] (© Dr. Jay Mehta's YouTube channel)

a) Insertion of the bag into the abdomen, b) Opening of the bag and placement of the specimen inside the bag, c) Closing of the bag, d) Removal from the abdomen

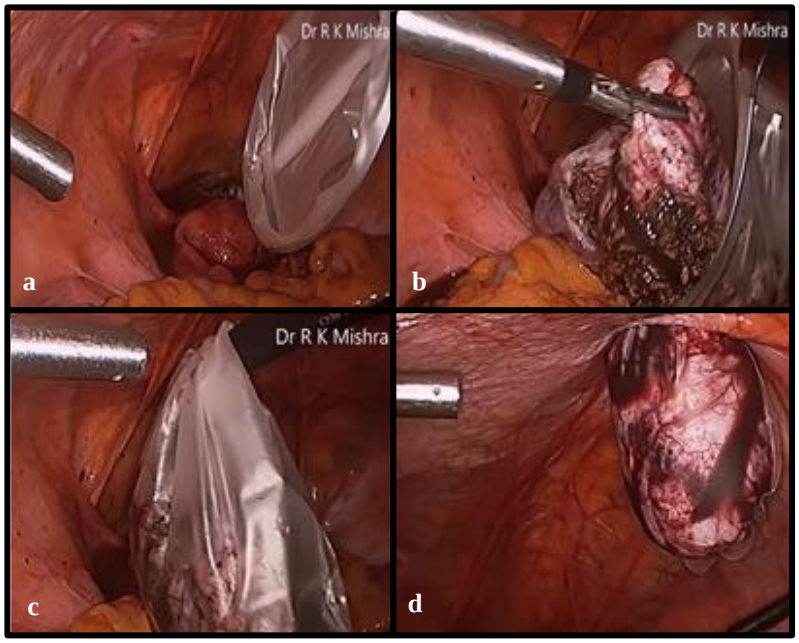

Fig. 7 Stages of specimen removal using an automatic bag [70] (© Dr. R.K.Mishra's YouTube channel)

a) Insertion of the bag into the abdomen. The bag is automatically deployed, b) Placement of the specimen inside the bag, c) Closing of the bag, d) Removal from the abdomen

2.4 Robot-Assisted Minimally Invasive Surgery

Robots were first introduced into the industry in the United States in 1961 [23]. Robots offer repeatability and more accuracy than humans do [24]. Robots have applications in other diverse fields ranging from agriculture [25] and aerospace [26] to education [27]. It has been nearly two decades since the first appearance of robots in operation theaters [15]. Integration of robots in the operation theaters has enabled or improved many MIS procedures [28]. Robotic surgery enables surgeons to operate with more precision due to motion scaling ability and various embedded motion sensors. In addition, robots bring an intuitive motion back to the operation rooms where they eliminate challenges such as fulcrum effect, inherent in traditional MIS. Robots can be built in miniature scales that can be delivered through small ports into the body cavity and enable certain new procedures that previously were either impossible or very arduous to perform. One of the most crucial benefits of using robots in surgery is the fact that the surgeons could operate the robots from a remote site far away from the patient. This is especially important for surgeries that require x-ray imaging during the procedure (e.g., catheter ablation where X-ray imaging is used to visualize the position of, and guide, the catheter inside the vascular system of the patient) [29]. The surgeon can be stationed in a remote site away from the harmful radiation and operate on the patient with high precision and control.

Fig. 8 Traditional laparoscopic surgery setup (left) [71] vs. Robotic-Assisted MIS surgery (right) [72]

Since the inception of surgical robotics, robots have evolved from autonomous systems to tele-operated platforms and mechanically-grounded, cooperatively-controlled robots [11]. In addition, hand-held robots have seen a significant development in the last decade. Most of the research in the last 20 years have focused on the development of mechanically-grounded and cooperatively controlled robots. The first surgical robot that obtained FDA approval for use in the operation rooms was the automated endoscopic system for optimal positioning (AESOP). The AESOP system consisted of a camera arm that mimicked the human arm movements, giving the surgeon full control over the camera system via a voice command or a direct foot pedal [30]. Similarly, another robotic system named TISKA was developed in Germany, which maintained a stable invariant point of constraint with the trocar puncture site that could be used as either an optical positioning device or an instrument retractor [31]. Other similar robots for use as assistive imaging systems were developed during late 90s in [32] and [33]. Table 2. depicts the advantages and disadvantages of Robotic-Assisted surgery versus conventional surgery.

Table 2. Advantages and Disadvantages of Robotic-Assisted surgery Versus Conventional Surgery (2004) [59]

Human strengths	**Human limitation**	**Robot strengths**	**Robot limitations**
Strong hand-eye coordination	Limited dexterity outside natural scale	Good geometric accuracy	No judgment
Dexterous	Prone to tremor and fatigue	Stable and untiring	Unable to use qualitative information
Flexible and adaptable	Limited geometric accuracy	Scale motion	Absence of haptic sensation
Easy to instruct and debrief	Limited ability to use quantitative information	Can use diverse sensors in control	Expensive
Rudimentary haptic abilities	Limited sterility	May be sterilized	Technology in flux
Able to use qualitative information	Susceptible to radiation and infection	Resistant to radiation and infection	More studies needed
Good judgment			

2.4.1 MASTER-SLAVE ROBOTS

Although developments of imaging systems were progressing at a fast pace, the manipulability of instruments in MIS was still an unsolved issue. In the early 90s, the concept of a master-slave tele-manipulator was developed [34]. The master-slave configuration enabled the robot to operate remotely from the surgeon who is operating it. In this configuration, the doctor controls the robot from an ergonomic master station placed either in the same room where the robot is located or in a remote place that shields the surgeon from certain hazards contributed with some operations such as X-ray radiation in cases of fluoroscopy. The movement commands are then transmitted from the master console to the slave console to which the robot manipulators are

attached. At the master console, the surgeon articulates two handle manipulators made to replicate the movements of the surgical instruments. Various sensors at the master station collect hand movements of the surgeon. Then, the master console sends off the processed movement data to the slave console. After receiving command data at the slave station, movements are scaled down to provide precise and controlled movement at the end-effector of the robot. The robot manipulators follow the same direction as the surgeon's hands, which results in an intuitive operation for the surgeons. US Federal government supported the development of the first tele-operated surgical robot, which was developed by Stanford Research Institute in 1990s [35]. Since then, many other master-slave platforms have been developed for different purposes. Among these systems da Vinci robot (Intuitive Surgical Inc.) and Zeus (Computer Motion Inc.) [36] were the first set of robots deployed for clinical use. The da Vinci system is the only remaining commercially available system capable of performing complex abdominal and chest operations [37].

Fig. 9 Two of the most widely used Master-Slave surgical systems [59]

a) da Vinci surgical system by intuitive Surgical. In this system, 3D stereoscopic image of the surgical site is displayed through goggles. b) ZEUS surgical system by Computer Motion Inc. This system provides stereoscopic images by polarized goggles. Left lens only shows the images captured by the left camera and the right lens only shows the images captured by the right camera.

2.4.2 COOPERATIVELY CONTROLLED ROBOTS

Recent developments of compliant surgical platforms that are able to seamlessly cooperate with the surgeons during the surgery, have enabled new possibilities for procedures that were previously considered impossible or very challenging to perform. The outcome is a new approach in robotic surgery primarily focused on a cooperative operation between the robot and the surgeons both pre- and intra- operatively. This approach dictates that the robot's priority should always be to keep the surgeon in the control loop, simultaneously sense, and adjust itself to the dynamical changes in the surgical workflow. Thus, the utilization of this method combines the superb human judgment ability with fine precision of robots to achieve tasks that are physically challenging to be done solely based off humans' natural abilities to function at micro scale precisions or are very challenging, if not impossible, to be fully automated to be done solely by the robots [38]. Some robots that have been developed for cooperative surgery are the Johns Hopkins "Steady-Hand" robot for retinal microsurgery [9] and ACROBOT for total knee replacement operation [10].

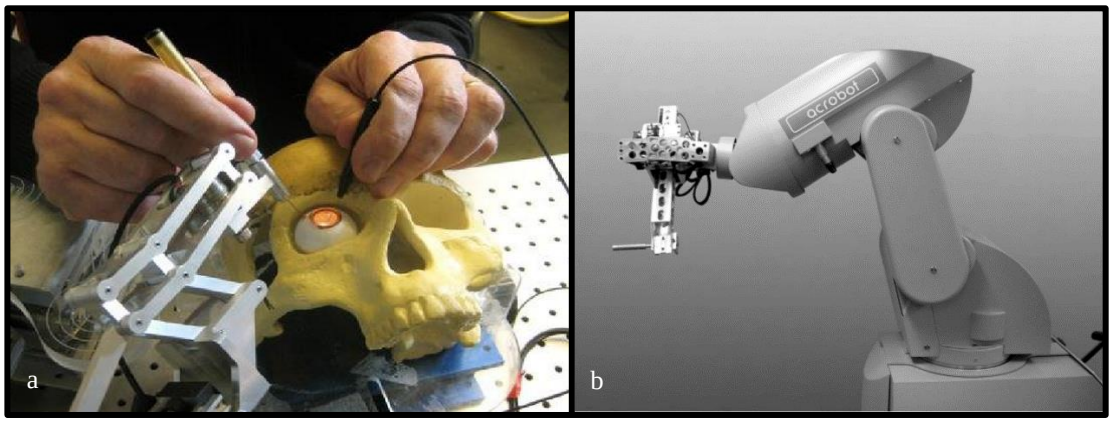

Fig. 10 Two example of cooperatively controlled robots [38, 10]

a) Steady-hand eye robot developed in Johns Hopkins University for retinal microsurgery. This device minimizes hand tremors by sharing the instrument control between the surgeon and the robotic manipulator, allowing precise and steady motion [38, 9]. b) Imperial college active constant robot (Acrobot). The system allows the surgeon to guide the manipulator under active constraint control that enables safe and precise machining of the bone surface [10].

2.4.3 HAND-HELD ROBOTS

Since the proposed design of this thesis lies in this category, the examples of the hand-held systems will be covered more in depth in this section. Although master-slave and cooperatively-controlled robots' progress in clinical applications has been impressive and noteworthy, the high costs of these systems, large footprint in the operation theaters and extensive learning curves for acquiring the necessary skills for operation of those machines are some of the prohibiting factors for more wide-spread use of those systems. These limitations have pushed the direction of research into new arenas to accomplish the tasks where high precision of the robots is required to overcome the physical limitations of manual manipulation of the instruments. One benefit to this approach is the compactness of these systems in comparison with the mechanically grounded surgical robots that enables the seamless integration of these systems with the normal workflow of the operation rooms with little or no setup time [11]. In addition, hand-held devices have significantly less cost due to reduced actuation DoF, sensors, and control units.

Hand-held robotic instruments for MIS or hand-held robotic manipulators, also called comanipulators are referred to as any type of robotic manipulators where an operator is in contact with the system and has direct control over the operation of the robot [39]. The goal behind the design of these systems is to improve the operator's manipulation performance by means of increasing the dexterity of the surgeon's movements and/or providing force feedback and force amplification to the surgeon [40]. The benefit to these systems is that by keeping the surgeon at the patient's side, the workflow of the operation room is not disturbed, and the patient can benefit best from the combined superb judgment abilities of the surgeon while benefiting from the assistive feature of the robotic system. Many works have been done in the field of surgical robotics to improve the intuitiveness of the teleoperation systems by providing force feedback and high

definition 3D stereoscopic images, but still the direct manipulation of the instruments remains the most instinctive and straightforward way to perform the surgery [40]. Handheld robots are divided into five classes based on the assistive features that they provide to the surgeons. These classes are: 1) *tremor suppression devices*; 2) *active guidance system*s; 3) *mechatronically-articulated devices*; 4) *force control systems* and (5) *haptic feedback devices* [11]. The following is a concise review of works that have been done in each of these classes.

2.4.3.1 Tremor Suppression Devices

The *Micron* designed by Carnegie Mellon University is an actively stabilized tool that increases the manipulation accuracy in microsurgery by eliminating the operator's unwanted tremor during the operation [41]. The undesired handle motion of the device is counteracted by the tool tip. The device is comprised of 3-DOF piezoelectric manipulator with 400-μm range of motion. An optical position-measurement subsystem is utilized to acquire the position and orientation of the tool tip of the device with 4−μm accuracy at 2000 samples/s. The feasibility of the device was proved by the testing of three eye surgeons and three non-surgeons that showed between a 32-52% reduction in the position error in the tooltip of the device.

Saxena et al. proposed a novel approach based on the use of Ionic Polymer Metallic Composites (IPMCs) for actively compensating physiological tremor in the hand [42]. The devise is composed of three parts: a sensor module at the distal end, a manipulator module at the proximal end and a body that attaches the sensor and the manipulator modules. The motion of the hand is measured by the sensor module in six degrees of freedom using two inertial measurement units. The tremor motion is then compensated by the information acquired from the sensor units resulting in filtering of the undesired motion of the tooltip of the device.

2.4.3.2 Active Guidance Systems

Song et al. presented a handheld Smart Micromanipulation Aided Robotic-surgery Tool (SMART) micro-forceps [43]. Fiber-optic common-path optical coherence tomography (CP-OCT) sensor is used for guiding of the tooltip. The tool tip position is manipulated longitudinally through a closed loop control using a piezoelectric motor. A novel forceps was designed to enhance the safety and efficiency of the operation. The results of the preliminary experiments showed significant improvement over the conventional freehand use.

2.4.3.3 Mechatronically-Articulated Devices

Isakov et al. designed and developed a laparoscopic power morcellator device with motorized mesh, which enabled contained morcellation of large excised specimens for laparoscopic surgery [44]. The device was consisted of two main components: 1) a modified morcellator with a protective blade cover, 2) a motorized retracting mesh for containment of the tissue during morcellation, which is hypothesized to greatly reduce dissemination of the cutting parts to the abdominal cavity. The device showed improvements in terms of speed over conventional morcellators.

Dario et al. presented a novel mechatronic hand held robot for arthroscopy [45]. The device has a cable-actuated servomotor-driven multi-joint mechanical structure, which is equipped with a position sensor measuring the orientation of the tooltip. Force sensors are used to detect possible contacts between the tooltip and the knee. The device demonstrated capabilities in controlled movements of the tip of the instrument based on surgeon’s commands and while preventing undesired contacts of the tooltip of the device with the knee.

2.4.3.4 Force Control Systems

Johns Hopkins University has developed a 3-DOF force sensing micro-forceps for membrane peeling in vitreoretinal surgery [46]. The device consisted of a modified commercially available micro-forceps that is actuated using a compact motorized unit. Four fiber bragg gratoring strain sensors were used to capture the force at the forceps in three degrees of freedom and feed them back to the surgeon. Tests were conducted to determine the repeatability of the force sensors reading of the device, which showed it to be within 2 pm. Further tests demonstrated that the proposed device could predict 3-D forces with an rms error under 0.15 mN in the transverse plane and within 2-mN accuracy in the axial direction.

Mirbagheri et al. designed a triple-jaw actuated and sensorized instrument for grasping large organs for MIS [47]. The Device benefited from a DC motor with encoder that enabled auto-grasping of large specimens during tele-operation surgeries as well as in onsite MIS as a hand-held robotic device. The opening mechanism of the triple-jaws was achieved by using a slider-crank mechanism where each jaw was comprised of two grasping segments. The device could effectively open to an 80mm diameter, which allowed the robot to grasp large delicate abdominal organs. Strain gauges where used in each jaw to provide the surgeon with the grasping force at the jaws.

Gafford et al. designed and developed a soft, atraumatic, deployable surgical grasper with on-board pressure sensing for grasping soft tissue during laparoscopic pancreatic surgery [48]. The fabrication of the grasper was achieved using shape deposition manufacturing with the pressure sensors embedded into each finger of the grasper. The grasper was comprised of three fingers, each 103 mm long and 14 mm outer diameter when closed. The grasper could be inserted to the abdomen through a 15 mm laparoscopic trocar and provided surgeon with compliant interface

between soft and delicate pancreatic tissue and the metal laparoscopic forceps which has the potential to reduce risks of hemorrhage.

2.4.3.5 Haptic Feedback Devices

Payne et al. presented a force amplifying hand held device for micromanipulation [49]. The device is capable of amplification of delicate micromanipulation forces up to 15 times. The amplified force is relayed back to the surgeon via a slider that is mounted on the handle of the device. A closed-loop force control scheme is used to perform the amplification of the sensed force. Instruments can be interchanged through a simple docking feature allowing the device to be used in a wide range of micro manipulation applications. The results have shown a five times reduction of the minimum force threshold perceived by the subjects and ergonomically sound manipulation advantages.

Yao et al. developed and enhanced a probe that could improve the tactile sensations experienced while probing objects [50]. The instrument consisted of an accelerometer and an actuator. To decouple input from output, those components were arranged in a way that the sensing direction was orthogonal to the actuating direction. The device demonstrated an ability to amplify the signals by 10 dB on average, which showed significant improvements in performance in the case of tactile and auditory feedbacks.

CHAPTER 3

3 ROBOCATCH: DESIGN CONSIDERATIONS

The proposed design attempts to overcome the existing issues of manual specimen retrieval in laparoscopic surgery by embedding a suite of motorized instruments into a hand-held robotic device that will be operated by a surgeon via an onboard joystick controller. The proposed hand-held robot is christened as RoboCatch, owing to its primary function of catching (cage-grasping) a specimen before it is retrieved. The core instrumentation of RoboCatch significantly modifies and extends conventional instruments that are currently used by surgeons for the retrieval task (laparoscopic grasping forceps and a specimen retrieval bag). In particular, the proposed instrumentation combines a pair of forceps and a grasper that are concentrically situated in a folded configuration inside the device's tube, which achieves the functionality of a conventional trocar:

1) **Actuated forceps:** A commercially available atraumatic laparoscopic grasping forceps is modified and integrated into the design to serve the purpose of retracting and placing the excised specimen into the specimen bag. The opening/closing of the forceps is achieved by using a cable-driven DC gear motor control mechanism.
2) **Webbed three-fingered grasper:** The grasper comprises a set of three robotic multi-jointed fingers with an angular separation of 120^{o} between each other. The fingers are attached to a flexible specimen bag by encompassing it from the outside. This arrangement enables the opening/closing of the bag by controlling the finger movements through a linear servo-control mechanism. The articulation in the fingers and the compliance of the bag enable the grasper to comply with the morphology of the excised tissue. The specimen bag is constructed out of a non-powdered surgical glove [51].

RoboCatch enables a surgeon to achieve the specimen retrieval task in six stages:

1) The main tube, serving as a trocar, is introduced into the surgical site through an instrument port
2) The three fingers slide out of the tube and simultaneously unfold, and open, in an umbrella like-fashion
3) The concentrically placed pair of forceps moves out of the tube toward the excised specimen and grasps the specimen
4) The forceps retracts the grasped specimen into the center of the grasper
5) Once the specimen is in place, the webbed three-fingered grasper closes onto it, resulting in a secured containment of the specimen
6) The grasper, along with the contained specimen, will be manually removed from the abdominal cavity.

The first step of the design process was to gather crucial parameters from the surgeons in the field, who could clearly point out the important features anticipated from a device like the one presented in this thesis. After thorough discussions with the surgeons, a design requirements table was created, which served as a guideline and a foundation on which the proposed design was based on. The table provided important information regarding the overall device dimensions, actuator selection, and the fabrication material that could be used for making the robot. The CAD models were developed in SolidWorks 2018 CAD modeling software. The actuation mechanisms were examined in a simulated environment within the CAD software in order to ensure their operability before the fabrication of the physical robot. The components of the robot structure were fabricated

using an Objet30 Prime 3D printer and assembled, with all the actuation systems embedded into the assembled robot structure.

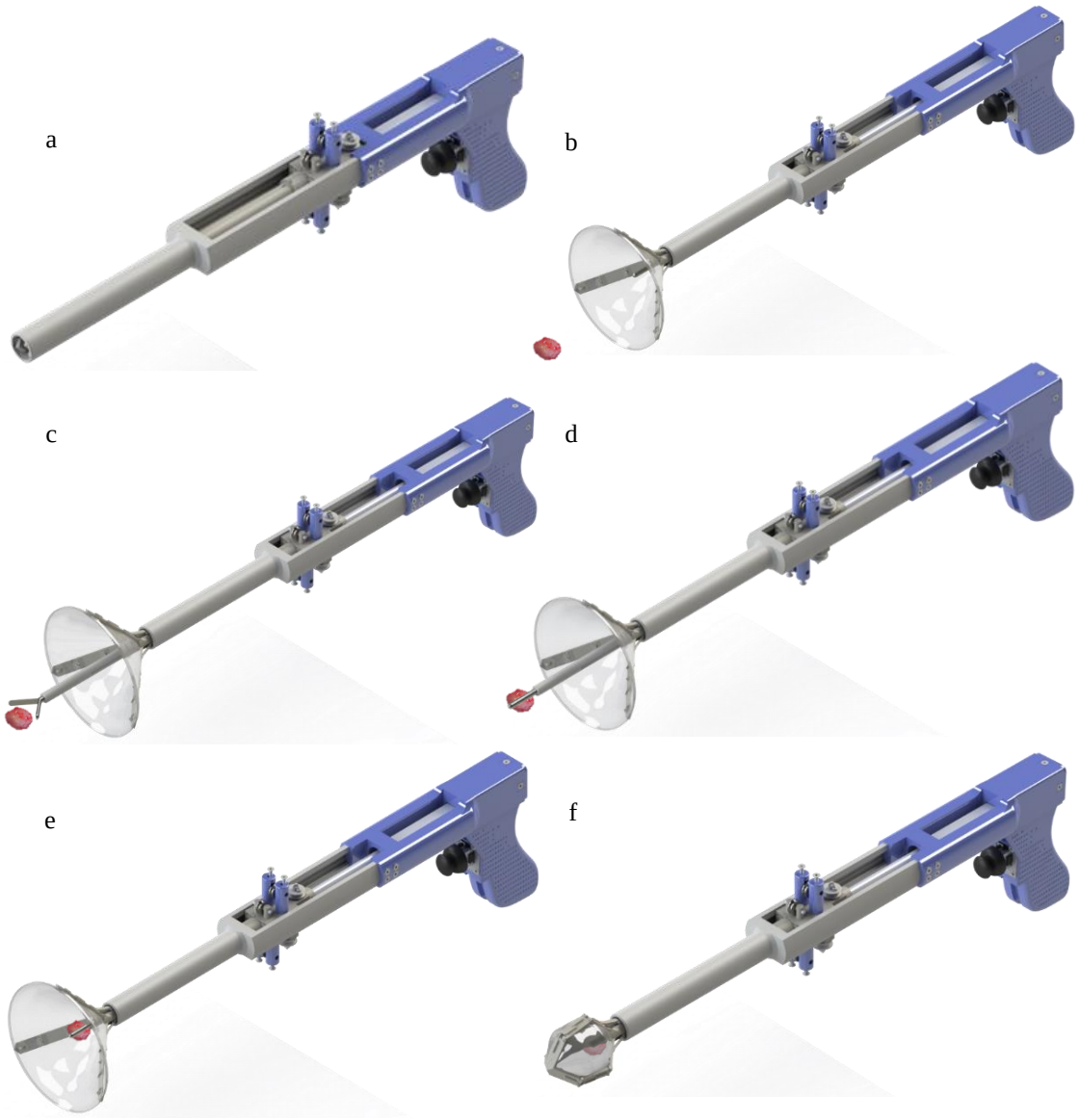

Fig. 11 Stages of specimen retrieval for the RoboCatch

a) The tube of the RoboCatch is inserted into the abdomen.b) The webbed three-fingered grasper slides out of the tube and unfold in an umbrella-like fashion c) The grasping forceps moves outside of the tube towards the excised specimen. d) The forceps grasps the specimen and retracts to the center of the webbed three-fingered grasper. e) The specimen is placed at the center of the grasper. f) The webbed three-fingered grasper close onto the retracted specimen. Finally, both grasper and the contained specimen will be remove from the abdominal cavity.

Table 3. Design requirement table versus the final products outcome

design parameters	Surgeons requirement	Final device measurements
Max weight	$\leq 600gr$	$540gr$
Max length	$\leq 600mm$	500mm
Main tube diameter	$\leq 15mm$	$20mm$
Tube length	$150mm$	$150mm$
Forceps type	Atraumatic	Atraumatic
Operation complexity	Simple on-board controller	Multipurpose Joystick controller
Material	Biocompatible	Biocompatible
Cost	< $1000	≅ $450

The following section will describe the design considerations that were taken into account. When designing a MIS robotic manipulator, the kinematics design of the robot is paramount to achieve a successful and practical product, with attention to crucial factors like system safety, ergonomics, motion constraints, system workspace, and mechanism topology. These design aspects are described below.

3.1 Motion Constraints

One motive behind utilization of robots for surgical operations is to benefit from their assistive features that they provide to the human operator. One of these features is the intraoperative assistance of the surgeon with an improved dexterity in movements of the surgical instrument. In a laparoscopic surgery, at least four-degree-of-freedom (DoF), including three rotational and one translational motion is required for the laparoscopic instrument to safely operate within the body [52]. Thus, for a robot to be used in a MIS, there are generally two motion constraints present. First, the robot should have at least 4 DoF to be able to manipulate the surgical

instruments. These motions can be characterized as roll, pitch, and yaw for the rotational motions of the robot and axial translation for the depth of insertion of the robotic tool inside the patient's body. These DoF allow the tip of the instrument to move freely inside the abdominal cavity without being stuck in a situation that it would be impossible for the instrument to set itself free. An in depth description of the length of the insertion along the tool's axis and the rotational movement about the pivot point can be found in [53,54]. Second, parts of the robot's body that are operating externally with respect to the patient's body, should not come in contact with the patient's body at any circumstances during its operation. [52]. This motion constraint ensures that the operation of the robot does not pose any hazards regarding the collision of the robot's mechanical links and joints with the patient during the surgery.

3.2 Safety

Safety is the number one concern in the operation rooms (OR). Protocols have been developed in order to provide clear guidelines for surgeons and technicians to avoid any unwanted complications that could potentially put the lives of the patients or technicians present in the OR in danger. One safety protocol dictates that, all instruments and tools present in the OR, should be sterilized and decellularized based on defined guidelines, prior to surgery [55]. Surgical robots are also bound to follow these protocols. Any part of the robot that could potentially come into contact with the patient's body or contaminate the surgical site, must be sterilized or covered with a sterile cover [53]. Additionally, materials that make contact with patient's body should not be causing any harmful chemical reactions while they are being used inside the body. These requirements imposed upon us to do a vigorous study on designing our robot in a way that all the components that make physical contact with the patient's body could be easily cleaned and sterilized after each operation. Moreover, we chose a biocompatible 3D printing material (VEROWHITE PLUS

RGD835 and VEROBLUE RGD840 manufactured by Stratasys Inc.) for the fabrication of all components of the robot. Hence, we eliminated any risks of adverse reactions of the patient's body with the robot while it is operating on the patient.

Other design considerations regarding the safety of the surgical robot arises directly from the motion constraints of the robot [52] discussed in the previous section. One factor states that the robot should not collide with the patient's body during its operation and the other one calls for a minimum of four or more DoF for the robotic instrument. This calls for a carefully thought out design that examines the motion of each joint and link of the robot and ensures a collision free operation. Lastly, the device's actuators should avoid unnecessary high-speed movements of the robot's manipulators [53]. Rigorous design analysis was done to choose the proper type of actuators that generate enough actuation force while not exceeding the safe operating speed threshold.

3.3 Ergonomics

Ergonomics is a science that takes into account the limits of the operator and enables designs that optimize the performance of the user [56, 57]. In a hand-held device such as our robot, ergonomics mainly relates to the ease of manipulation of the device. The determinant factors that directly correlate with the manipulability of the device are the overall dimensions of the robot, total weight of the device, and design of the robot's handle. Hence, in the design process our aim was to minimize the weight of the RoboCatch, while retaining the structural rigidity of the system intact. Moreover, the actuation units were selected in a way that they would occupy the least amount of space in the system and yet provide an adequate amount of force for the actuation of the mechanisms of the robot. Guidelines regarding the design of the handle of a hand-held device based on an average measurements of human hands were studied and utilized for the most

comfortable and ergonomic design[58]. The width of the handle was selected to be 30 mm so that it would be suitable for both female and male operators. The length of the handle is approximately 110 mm, which closely complies with the literature guideline that suggests the ratio of handle diameter to length to be 1:4. Additionally the slope of the handle is set to 60° to provide a comfortable grip for the surgeon during the operation of the robot. The average hand measurements are provided in Table 4.

Table 4. Average hand dimensions [58]

Gender	Item	Measurements(mm)
Male	Hand length	187.9
	Hand Breadth(four fingers)	83.6
	Grip breadth inside width diameter	44.5
	Grip breadth inside width diameter	35.6
Female	Hand length	167.9
	Hand Breadth(four fingers)	75.2
	Grip breadth inside width diameter	32.2
	Grip breadth inside width diameter	25.7
Average	Hand length	177.9
	Hand Breadth(four fingers)	79.4
	Grip breadth inside width diameter	38.3
	Grip breadth inside width diameter	30.7

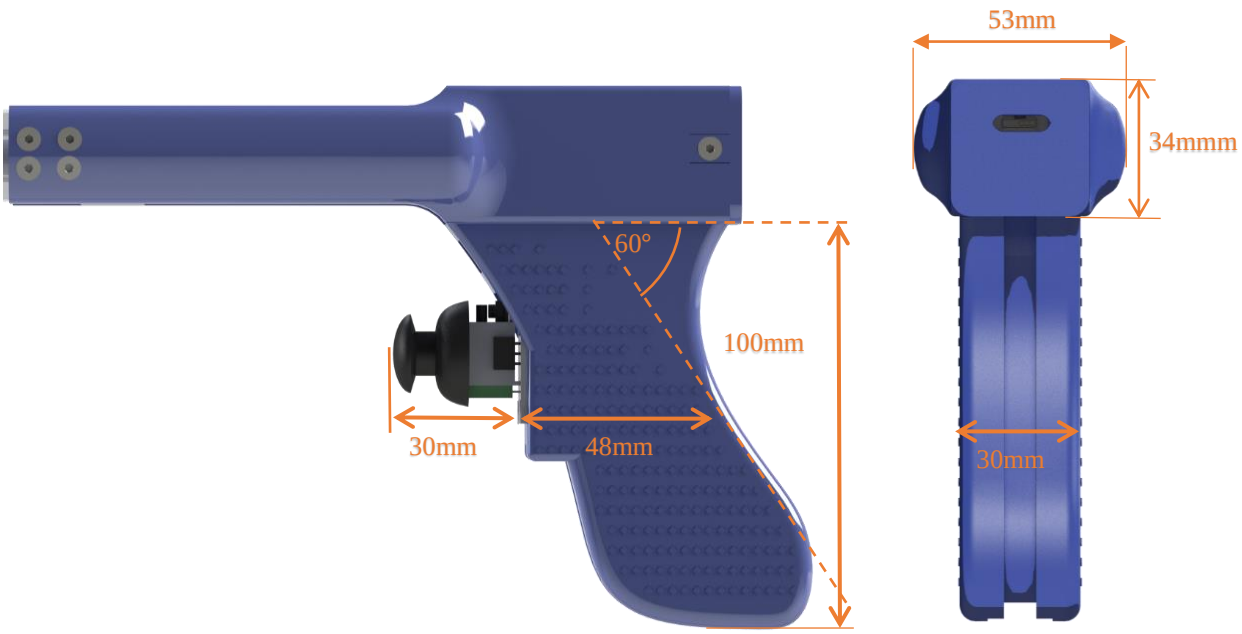

Fig. 12 Handle design parameters

3.4 System Workspace

Robot's workspace refers to the set of all points in a volume of space that can be reached by the robot's end-effector. For a solution to exist, the specified goal point must lie within the workspace of the robot. In the design of a surgical robot, it is crucial for the end effector to be able to reach any desired point within the operation site. In design phase of our robot, the measurements for the intra-body working parts were carefully chosen to ensure that the robot possesses an adequate workspace to successfully perform its intended task. RoboCatch has five DoF excluding the opening and closing of the grasper. Four DoF are considered to be the same as the conventional laparoscopic instrument and the additional DoF is for the axial translation of the forceps inside the middle tube that allows the robot to reach to the excised specimen and bring it to the center of the specimen bag. Thus, the workspace of our robot creates a spherical conic shape that represents all the points in space that the robot can reach during its operation. The entry point where the robot

enters the body acts as the pivoting point that limits the lateral movement of the robot. Thus, the vertex of the spherical cone is considered to be at the entry point and its height R would be the total distance from the entry point to the tip of the grasper in its fully extended configuration. Therefore, the volume of this cone can be calculated as the following:

First the surface area of a spherical cone should be calculated using the following formula:

$$A_{zone} = \pi R(2h + a), \qquad (1)$$

Where **A** is the surface area of the spherical cone and ***a*** is the horizontal distance from the center to the outer edge of the cone. ***R*** is the maximum distance from the pivotal point to the tip of the grasper at its fully extended configuration and is equal to 250 mm. $\boldsymbol{\theta}$ is the maximum rotation angle of the instrument shaft about the pivotal point and is equal to 70°. ***h*** is the vertical distance from top of the base of the spherical cone to its edge. In order to calculate the surface area, first ***a*** and ***h*** should be calculated.

$$a = sin\theta * R \rightarrow a = sin70 * 250 \cong 235\ mm \qquad (2)$$

$$h = R - cos\theta * R = 250 - cos70 \cong 165\ mm \qquad (3)$$

$$A_{zone} = \pi * 250 * (2 * 165 + 235) \cong 443750\ mm^2$$

Then, the volume of the spherical cone **V**, which is equal to one third of the product of the area of the zone and the radius of the sphere, can be calculated:

$$V = \frac{1}{3}A_{zone}R = \frac{1}{3} * 443750 * 250 = 3697916\ mm^3 \cong 3698\ cm^3 \qquad (4)$$

So, the robot's workspace is calculated to be 3698 cm^3.

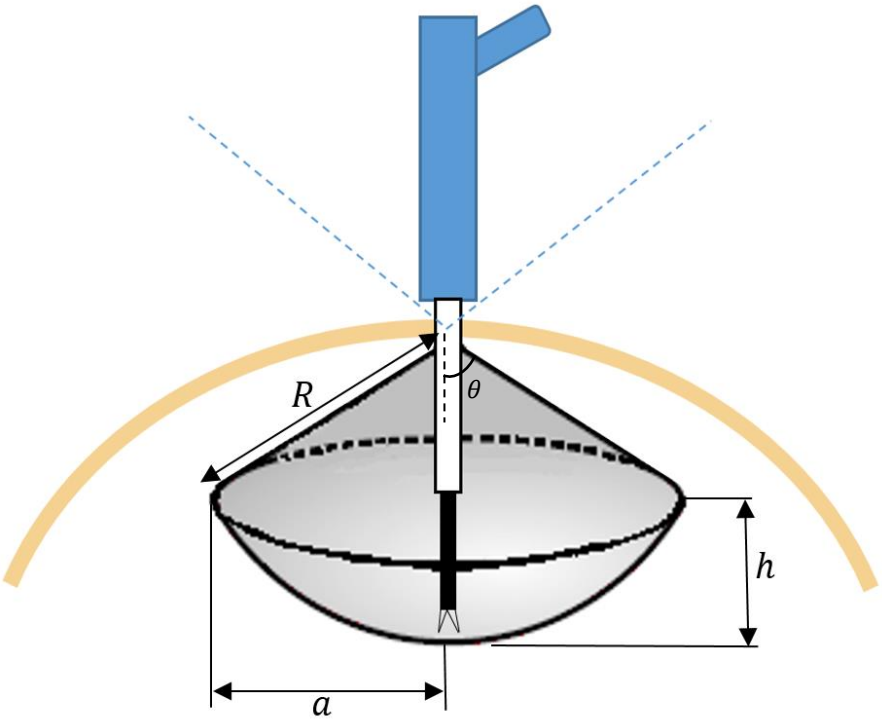

Fig. 13 Schematic of workspace of the RoboCatch

3.5 Material

Materials selection is considered an important phase in the design process of a medical device. Proper material properties is essential for having a rigid and reliable structure, ensuring that the device would withstand the forces and moments exerted on it during its operation. Additionally, the chemical properties of the selected material should be in accordance with the regulatory safety standards such as biocompatibility, sterilizability, and cleanability. The majority of our robot's parts have been made using additive manufacturing technique. A high-resolution Polyjet 3D printer (Objet30 prime, manufactured by Stratasys Inc.) was used for fabrication of the parts. Parts were printed using two different materials. VEROWHITE PLUS RGD835 (Stratasys Inc.) was used for fabrication of all parts except for the handle of the device and tensioners. VEROBLUE RGD840 (Stratasys Inc.) was used for the construction of the handle and tensioners.

Both of these materials are biocompatible and suitable for use in the medical devices. The advantage of VEROWHITE PLUS in comparison with VEROBLUE is that it provides more accuracy for printing small parts, and has slightly higher rigidity. These features are ideal for printing miniature sized parts that require high stiffness and submillimeter accuracy. This material is also preferred for printing parts with interlocking mechanism that are mated together with tight tolerances.

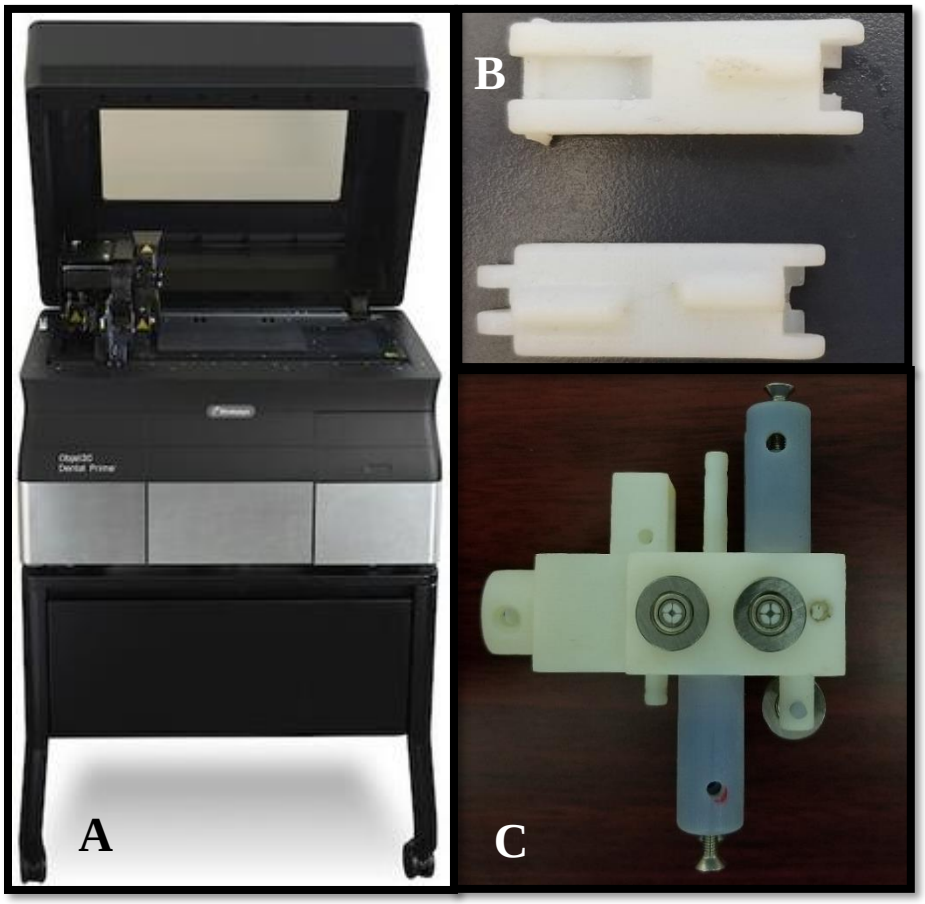

Fig. 14 Stratasys Objet30 Prime 3D printer and sample printed parts using two different materials

Stratasys Objet30 Prime 3D printer was used to fabricate components of the device with accuracy of 0.1mm. a) Stratasys Objet30 Prime 3D printer. b) Proximal and middle links of the webbed three-fingered grasper printed using VEROWHITE PLUS. c) Motor housing unit printed using VEROWHITE PLUS and tensioners printed using VEROBLUE.

Table 5. Material properties 3D-printed parts of RoboCatch

Material / Material properties	VEROBLUE RGD840	VEROWHITE PLUS RGD835
Tensile Strength (psi)	7250-8700	7250-9450
Modulus of Elasticity (ksi)	290-435	290-435
Flexural Strength (psi)	8700-10200	11000-16000
Flexural Modulus (ksi)	265-365	320-465
HDT (F°)	113-122	113-122

CHAPTER 4

4 ROBOCATCH: DESIGN, CAD MODELING, AND 3D-PRINTING

Crucial design requirements regarding the overall dimensions of the device, actuator selection, and appropriate fabrication materials were collected from the surgeons and used to generate a design table of RoboCatch, as presented in Chapter 3. In this chapter, we provide details of the design, CAD modeling, and 3D-printing of RoboCatch. We discuss the design, fabrication, and assembly of each component/mechanism and illustrate how it functions in the overall system. Actuation and control schemes are also covered in this chapter. The overall design underwent several iterations throughout the design process prior to finalizing the current design. The proposed device comprised of the following main components:

(1) 3D-printed body elements
(2) Webbed three-fingered grasper
(3) Modified atraumatic laparoscopic grasping forceps, and
(4) Control and power units

A combination of linear actuation and tendon-driven actuation is utilized to achieve the desired motion of the components. Deployment of the webbed three-fingered grasper and the axial movement of the grasping forceps are accomplished by the use of linear actuators and closing of the webbed grasper and the grasping forceps are carried out by the use of a tendon-pulley mechanism. The surgeon can provide motion commands by using an onboard dual-axis joystick controller (FICBOX Inc.). The joystick command signals are input to a microcontroller board (Arduino MEGA 2560 R3) and fed into the control program. The output signals from the microcontroller are sent out to the actuators.

4.1 Handle

Ergonomics of the handle is an important aspect in manipulation of a hand-held robotic device as the handle is the only robot's part that is in direct contact with the surgeon during the surgical operation. Ergonomics principles were used to create a design that is comfortable to hold for both male and female users and does not put excessive tension on the wrist of the operator. Average human hand sizes based on the available data in the literature [58] were used to help with determining the overall dimensions of the handle. A hollow handle structure was designed to reduce the overall weight of the device. This also enabled us to route the wires of the onboard motors through the opening of the handle, which helped with minimizing the interference of wires with surgeon's hand while operating the device.

The overall mechanical structure of RoboCatch is formed by the main tube frame and the handle. The rest of the components are embedded within either of these two parts. The overall configuration of RoboCatch is shown in Fig. 15. Three components are mated with the handle:

(1) Main tube frame, which is fitted into the slot at the front of the overhang part of the handle and secured using four flat head stainless screws on each side

(2) Joystick controller, which is positioned in front of the handle and controlled by the index finger of the operator

(3) Linear servo actuator, which is responsible for the deployment of the fingered grasper and housed at the top of the handle. A cap is attached to the back of the servo motor housing to secure the linear motor. The handle is designed with a diamond textured-surface to improve the contact friction between the handle and the surgeon's hand [1].

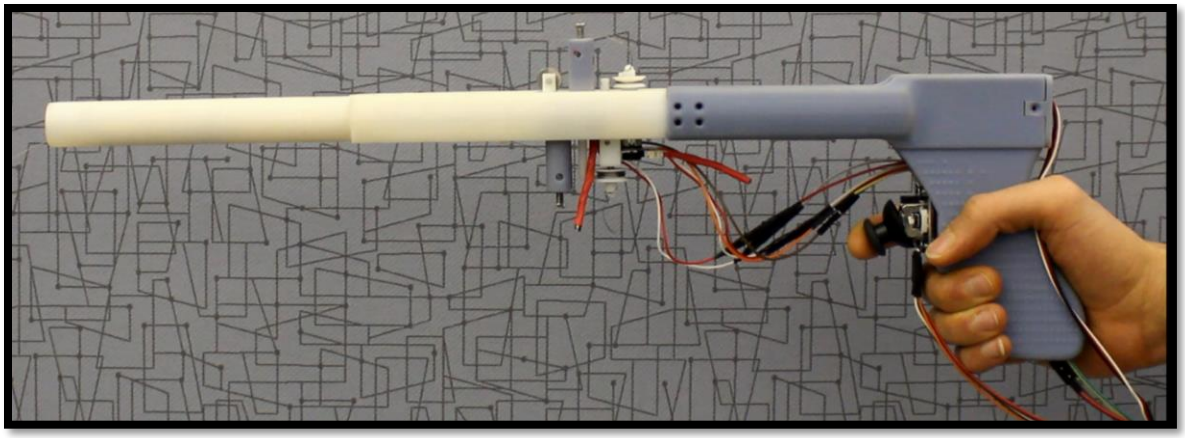

Fig. 15 Overall configuration of the RoboCatch

The handle was designed based of the ergonomics principles to provide comfortable handling of the device. The joystick controller is controlled by the index finger of the operator.

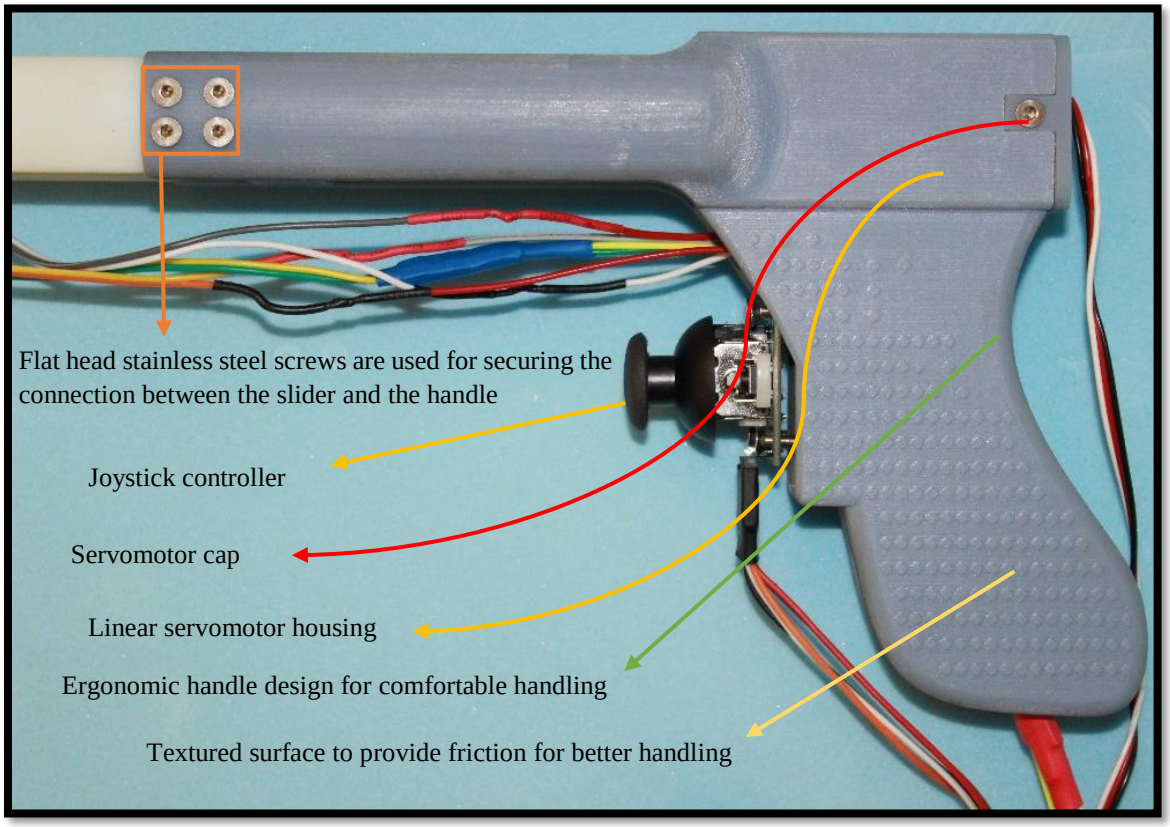

Fig. 16 Handle of the RoboCatch

Wires are routed through the hollow passage of the handle to prevent interference of wires with surgeon's hand. The index finger of the surgeon controls the joystick. The linear servomotor is housed at the top of the handle where it pushes the motor housing unit forward that results in the deployment of fingers out of the main tube.

4.2 Main Tube Frame

This component is comprised of two conjoined parts: a main tube and a linear rail. The main tube is the portion of the robot that is inserted inside the abdomen wall. The main tube functions as the trocar for the device, which keeps the incision port open and delivers the robot's instruments to the surgical site. Inside the main tube, webbed grasper and the grasping forceps are located. The webbed grasper is attached to the middle tube, and the grasping forceps are connected to the forceps tube. The main tube together with the middle tube and the forceps tube are concentrically mated within each other, creating a telescopic structure. In this configuration, the outermost layer is the main tube, with the middle tube positioned at the mid layer and the forceps tube at the innermost layer. Telescoping movement of the middle tube and the forceps tube is achieved by the use of a servo linear actuator. The linear actuator at the handle has an extending rod that is connected to a component called motor housing unit (MHU) which is mounted on the linear rail of the main tube and can slide along inside of it. The middle tube and the forceps tube are coupled to the font of the MHU. Thus, when the MHU is pushed forward, both the grasper and the forceps tube will advance through the main tube until the webbed three-fingered grasper is fully deployed out of the main tube. Thus, the first actuation stage of RoboCatch is completed with this action. Later (section 4.4), we provide more details on the deployment mechanism of the webbed three-fingered grasper. Assembled CAD model of different components of the device is shown in Fig. 17.

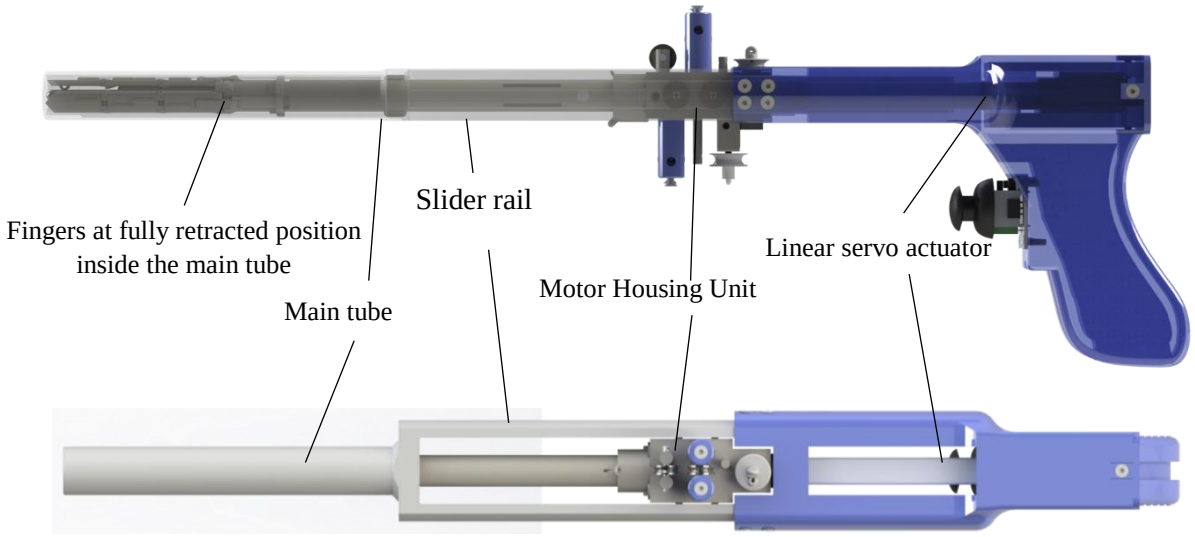

Fig. 17 Side and top view of the RoboCatch

at its retracted position. In the side view the main tube frame has been made transparent so that its inside components could be seen.

Fig. 18 Assembly of parts mounted on the main tube frame

4.3 Webbed Three-Fingered Grasper

One important feature of RoboCatch is its integrated specimen bag that allows for safe containment and removal of the excised specimens from the abdominal cavity. Different

laparoscopic surgeries deal with different types of tissues and organs. Therefore, types and sizes of the resected tissues vary greatly in each operation. Our device should be able to protect the integrity of the excised tissue and the specimen bag by absorbing axial traction forces that are applied to it from the excision port and the weight of the specimen, and spreading them throughout the device joints and links. The size and shape of the links should be selected in a way that allow for the compression of the volume of the specimen in order to minimize the need for enlargement of the excision for the removal of the specimen from the abdomen. Additionally, the bag needs to be completely sealed after the specimen is successfully retracted to its center. Finally, the device should allow monitoring of the whole process of retraction, containment, and removal of the specimen by the endoscope and refrain from obscuring the view of the surgical site.

In our device, the specimen bag is attached to a three-fingered grasper and is initially positioned in a folded configuration inside the device's tube. Having three segments for each finger enables the robot to comply with diverse sizes and types of retracted specimens. This configuration allows cage-grasping of the specimen and provides protection against the forces exerted on the specimen bag, while removing the device through the incision port. This eliminates the risk of the specimen bag rupture during the extraction stage and helps preserve the specimen's pathology for further examinations.

The specimen bag is made from a modified non-powdered latex surgical glove with its fingers removed. One end of the bag is attached to the distal segment of each finger with a purse-string suture around the bag's opening. The other end of the bag is attached to the proximal segment of the finger using a medical device adhesive (LOCTITE 013® Prism™), leaving only a small hole for passage of the grasping forceps. A seven-strand stainless steel cable with a diameter of 0.018 in was used for attaching the bag to the grasper using a purse-string suture. The cable was

connected to a pulley that was mounted on the shaft of the brushed DC motor. This motor is placed face down inside a motor housing unit (MHU). Cable tension is adjusted using the tensioner on the MHU to remove any slack in the cable.

The cable is inserted inside the middle tube and runs through grooves created on the segments of one of the fingers of the grasper. The cable is then passed through the distal segment of that finger and the distal segments of the other two fingers, while it weaves through the periphery of the specimen bag. The cable is looped back and attached to the starting distal segment, creating a looped knot. When the DC motor is activated, the cable is wound around the pulley, resulting in the closing of the fingers and tightening of the specimen bag.

Fig. 19 Modified surgical glove used in the webbed three-fingered grasper of RoboCatch

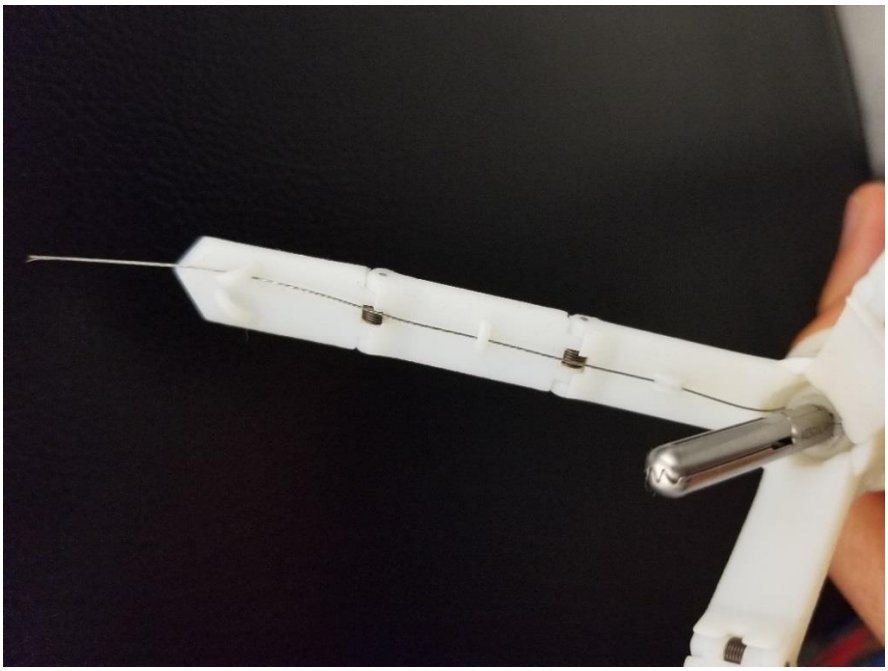

Fig. 20 Cable routing of the webbed-three fingered grasper

The stainless steel cable is routed through links one, two, and three of one of the fingers of the grasper. From link three, the wire starts a loop by passing through the specimen bag opening with a purse-string suture and the other third links of the grasper. The end of the cable returns to initial starting position of the loop and is tightened to the third link creating a looped knot. DC motor retracts the cable resulting in closure of the fingers and tightening of the specimen bag.

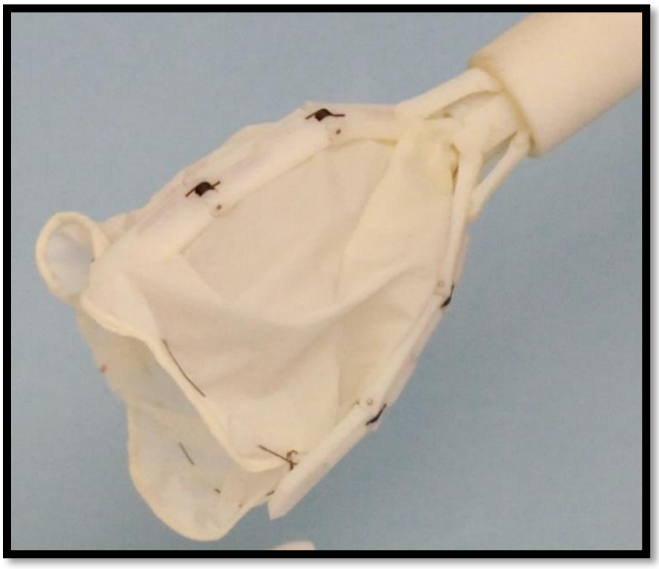

Fig. 21 Webbed three-fingered grasper

The specimen bag is attached to the fingers of the grasper with purse-string suture around its opening that functions both as an attachment of the bag to third links of the grasper and as a closing mechanism for the specimen bag.

After the insertion of the tube inside the body, the grasper fingers slide out of the main tube, and are simultaneously opened to a 55-degree angle with respect to the main tube's axis. The opening mechanism of the grasper is inspired by an offset slider-crank mechanism. Each proximal segment is attached to a slider ring via a coupler link. The slider ring has a linear motion constrained between two points on the middle tube. At one end, when the slider ring is at its farthest distance from the proximal segment's joint, the coupler link lifts the proximal link to a 55-degree angle, thus, providing the opening of the specimen bag and the grasper. When the slider ring is at its closest distance to proximal segment's joint, the coupler link pushes the proximal link down to a folded configuration, which is approximately parallel to the main axis of the main tube, allowing the grasper to be retracted inside the main tube. The opening of the grasper is achieved only when the forward motion of the slider ring is arrested, while the middle tube is advancing. In order to achieve this action, we created three longitudinal grooves at the interior walls of the main tube, each at 120-degree angle apart from each other. The slider ring had a matching extrusion with the grooves on its surface that allowed smooth sliding of the middle tube along the main tube. However, the grooves end at a specific distance from the tip of the main tube. Hence, when the middle tube reaches to a certain position outside of the main tube, the slider ring would make contact with the end of the grooves and stops moving forward. However, the middle tube continues its advancement, until the slider reaches its final stroke position. During this motion, the connecting links start lifting proximal link upward until the middle tubes stops moving. The maximum opening of the fingers is selected to be 55-degrees. This amount of opening provides enough volume to entrap most specimen sizes, while preventing it from excessive opening of the finger that would cause collision with other organs or abdomen wall.

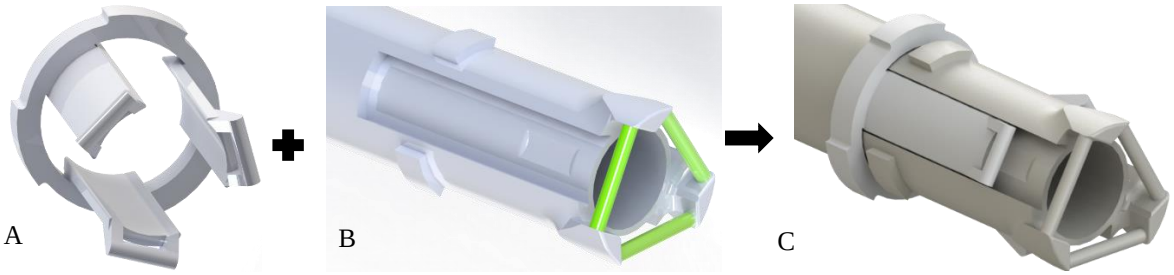

Fig. 22 Assembly of slider and the middle tube

A) Slider ring, B) middle tube tip, C) Mated configuration of slider ring and the middle tube. The slider ring has a constrained movement on the middle tube.

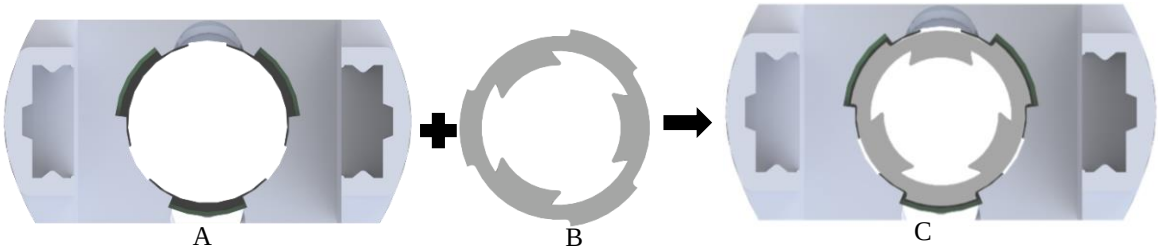

Fig. 23 Back view of the slider ring inside the main tube

A) The view of the back of the main tube; grooves can be seen on the interior side of the tube. B) Back view of the slider ring; Extrusions can be seen on the surface of the ring. C) The view of the mated configuration of the slider ring inside the main tube. Slider ring can freely slide along the length of the tube before reaching to the end of the groove.

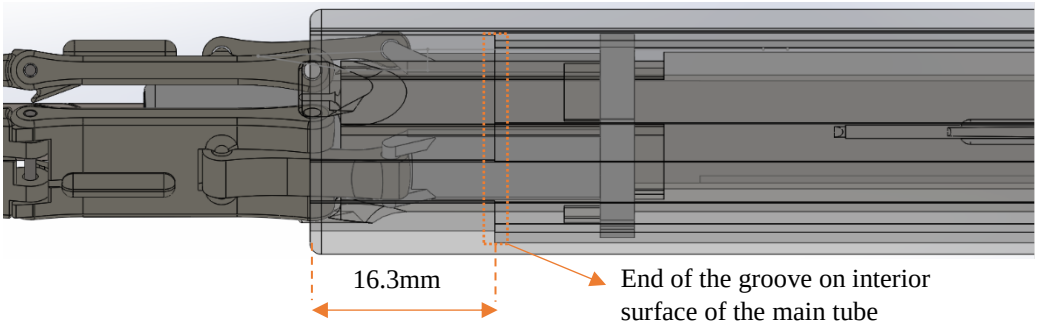

Fig. 24 Side view of the main tube and the middle tube

The groove ends at approximately 16.3mm from the tip of the main tube. After the slider ring has reached the end of the groove, the middle tube advances for an additional 2.6mm. This distance is called the stroke length of the slider ring. This additional movement provides the opening of the grasper.

The linear motion of the middle tube is provided by a linear DC servomotor, and is indirectly used for the actuation of slider-crank mechanism. The main goal of the linear DC

servomotor in RoboCatch is the deployment of the fingers outside of the main tube of the device. However, by utilizing the crank-slider mechanism, we were able to benefit from this linear motion by converting it into an angular motion of the fingers of the grasper. This design obviated the need for using separate actuators for controlling the opening and closing of the fingers. This resulted in less design complexity, lighter weight, more compact size, and lower cost for the device. The position analysis of the offset slider-crank mechanism of the RoboCatch is provided in the following:

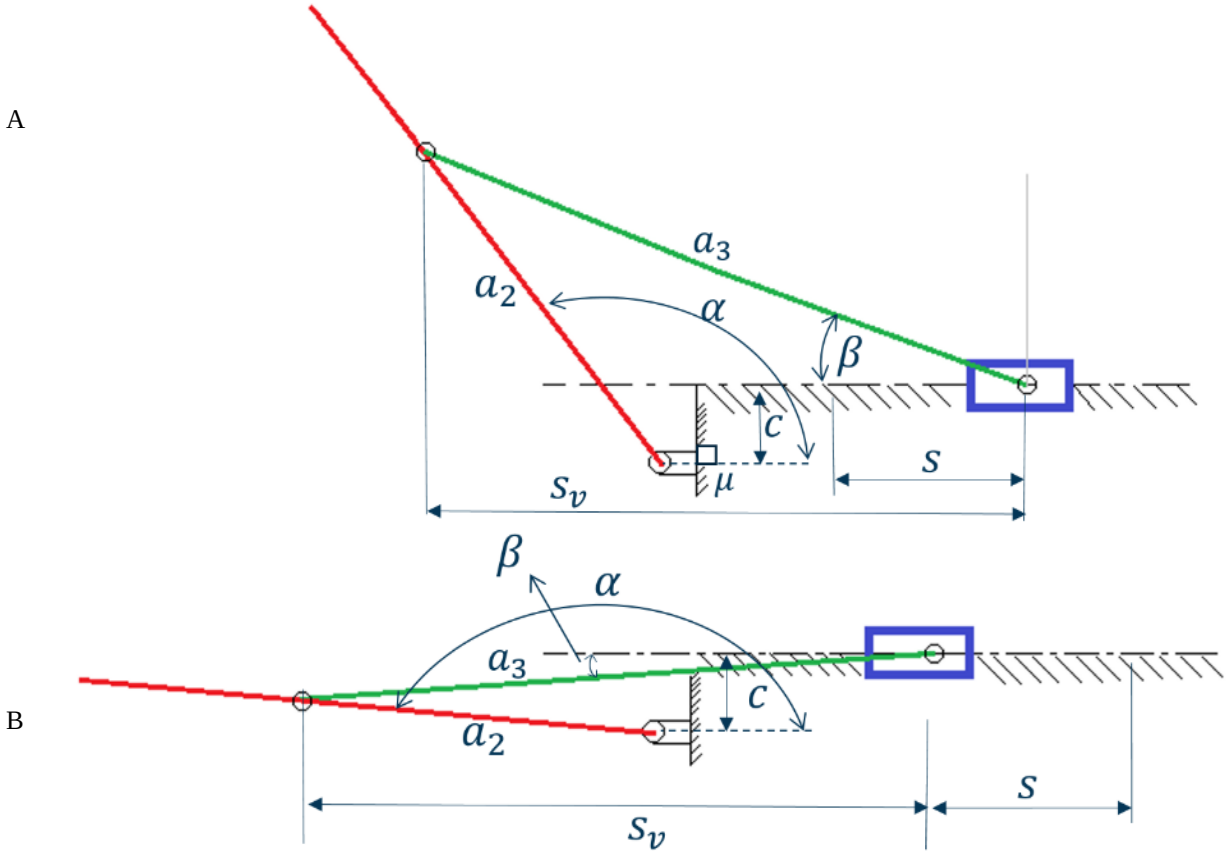

Fig. 25 Schematics of the offset slider-Crank mechanism of the RoboCatch

A) The slider ring is at its farthest position from the proximal link joint. Proximal link is lifted to a 55° angle with respect to the device's main tube axis. B) Slider is at its closest position from the proximal link's base joint. This causes the connecting link to push the proximal link of the grasper down, to an approximately parallel orientation with the axis of the main tube.

Table 6. List of notations for Fig. 25

Notation	Name	Minimum value	Maximum value
α	Angle between proximal finger and x-axis	124.44°	171.16°
μ	Angle between x-axis and offsset c	90°	90°
λ	Angle between s_v and x-axis	0°	0°
a_3	Connecting link length	14.93mm	14.93mm
a_2	Distance from the finger joint to the connecting link –finger joint	8.08mm	8.08mm
c	eccentricity	1.82mm	1.82mm
s	Stroke length	2.62mm	2.62mm
s_v	Distance of the slider-finger joint from the slider base joint	6.93mm	9.55mm
β	Angle between connecting link and x-axis	-2.22°	18.94°

Kinematic analysis of the mechanism:

Position equations:

$$a_2.cos\alpha + a_3.cos\beta + s_v cos\lambda + c.\cos\mu = 0; \quad (5)$$
$$a_2.sin\alpha - a_3.sin\beta + s_v sin\lambda - c.sin\mu = 0; \quad (6)$$

Constants: $a_2 = 8.08mm\,, a_3 = 14.93mm\,, c = 1.82mm, \lambda = 0,\ \mu = 90;$

$$8.08 * cos\alpha + 14.93 * cos\beta + s_v = 0;$$
$$8.08 * sin\alpha - 14.93 * sin\beta - 1.82 = 0;$$

Position analysis:

For a given finger angle α, position equations will solve for β and s_v . For the fully raised state of the proximal link where α=124.44:

$$8.08 * cos124.44 + 14.93 * cos\beta - s_v = 0;$$
$$8.08 * sin124.44 - 14.93 * sin\beta - 1.82 = 0 \rightarrow \beta \cong 18.94°;$$

Now by solving the first equation, s_v can be calculated:

$$8.08 * cos124.44 + 14.93 * cos18.94 - s_v = 0 \rightarrow\ s_v \cong 9.55mm;$$

For the closed state of the proximal link, α=171.16°:

$$8.08 * cos171.16 + 14.93 * cos\beta - s_v = 0$$

$$8.08 * sin171.16 - 14.93 * sin\beta - 1.82 = 0 \rightarrow \beta \cong -2.22°$$

Now solving for the first equation, s_v value is calculated:

$$8.08 * cos171.16 + 14.93 * \cos(-2.22) - s_v = 0 \rightarrow s_v \cong 6.93mm$$

Now to find the total stroke length, the difference of the maximum and minimum state is calculated:

$$s = s_{v@124.44} - s_{v@171.16} \rightarrow s = 9.55 - 6.93 = 2.62mm \qquad (7)$$

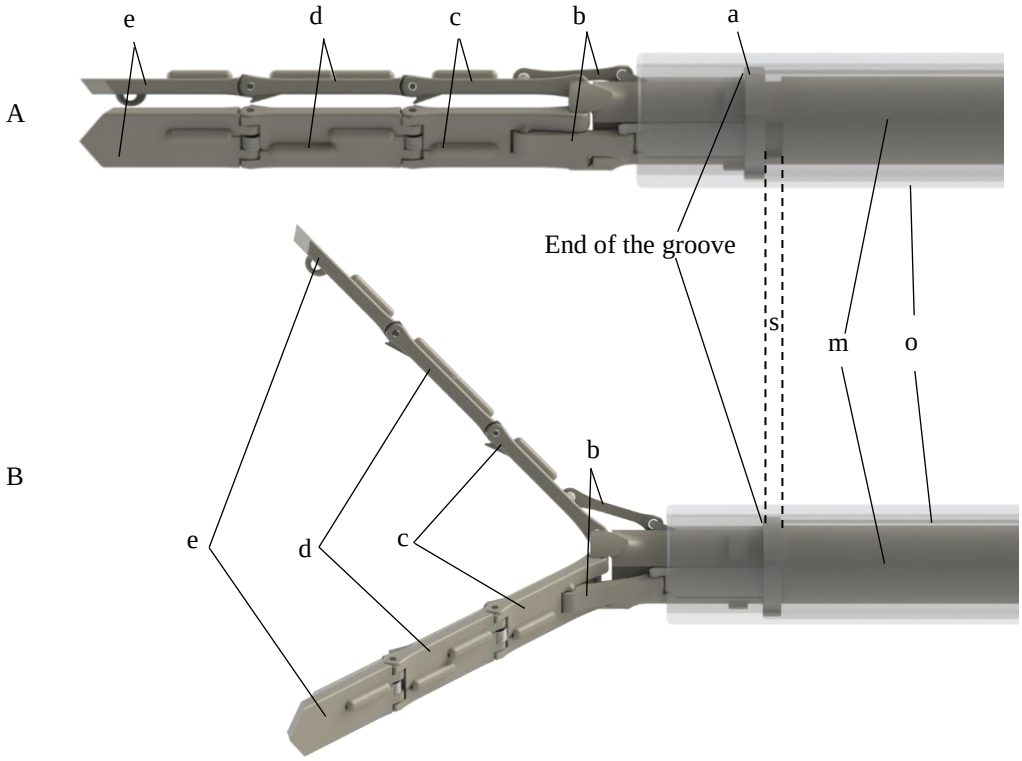

Fig. 26 Three-fingered grasper in folded (A) and unfolded (B) configuration

a) Slider ring, b) Connecting link, c) Proximal Link, d) Middle link, e) Distal link, s) Slider stroke, o) Main tube, m) Middle tube. Once the middle tube reaches to a certain position outside of the main tube, the slider ring will make contact with the end of the inside the main tube, which arrests its forward motion, however, the middle tube continues to advance. The distance from which the middle tube travels without the slider ring is equal to the stoke length of the slider. This will make the connecting link to stop its forward motion and lift the proximal link of the grasper to a certain predefined angle.

One novelty present in the design of our slider-crank mechanism is that all parts including: proximal links, connecting links, slider ring, and the middle tube were designed and fabricated as a single interconnected part with moving components. We achieved this design by benefiting from a key feature of the Objet30 prime 3D printer, which is its ability to print parts with tolerances up to 0.1mm. This superb accuracy offers completely new possibilities in the design and fabrication of intricate parts. The reason we chose this design and fabrication technique over the more conventional CNC machining, is that it would have taken us tens if not hundreds of man-hours to machine them and still, the accuracy of the finished parts would not have been as high as the 3D printed parts. After the fabrication of the parts, the support material needed to be removed so that the moving parts could move freely. To remove the support material, the part was placed inside a cleaning pool filled with cleaning solution consisting of 2% sodium hydroxide and 1% sodium metasillicate. After 18 hours of wash cycle, all support materials were removed from the part and the mechanism could move smoothly without any obstruction of support materials.

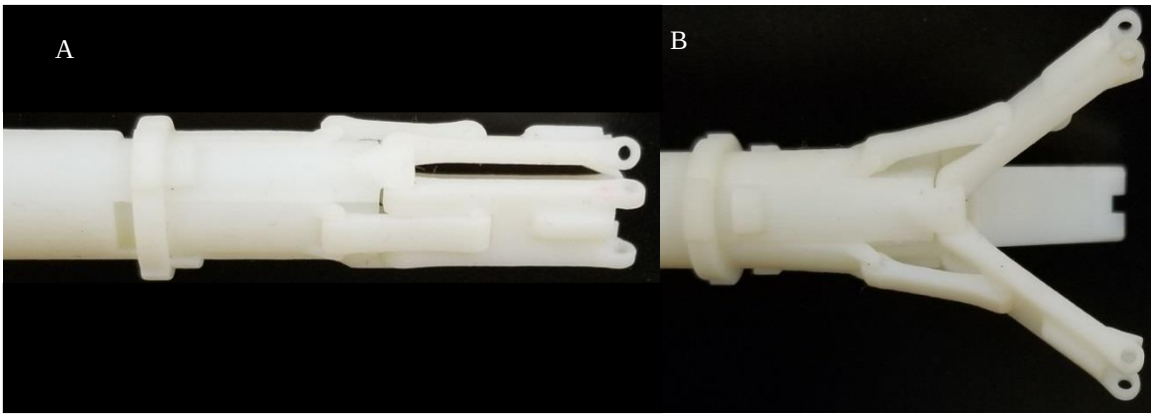

Fig. 27 Fabricated interconnected slider-crank mechanism of the RoboCatch

The mechanism consists of eight parts (3× proximal link-3×connecting link, middle tube, slider ring) and is fabricated using Objet30 Prime 3D printer. A) Folded configuration of the proximal link. In this state slider ring is in its closest distance from the joint of the proximal link. Proximal links are in a parallel position with respect to the main tube. B) Fully opened state of the proximal links of the grasper. The slider ring is at its farthest distance from proximal links' joint.

1mm stainless steel pins were used to attach the finger segments to each other. A 180-degree torsion spring was placed at each joint. The legs of each spring was fitted inside sleeve-like slots created on top of each finger. So that each spring would be connected to two links at each joint. Additionally, the inner loop of each spring was fixed with the pins at each joint. These springs provided moments required for lifting links two and three to a collinear position with link one. Thus, when fingers slide out of the main tube, all three links of each finger would be in a straight line. Hence, when the mechanism lifts the proximal finger, all links would deflect to the same angle as link one. This opening mechanism resembles an umbrella-like structure when fully unfolded.

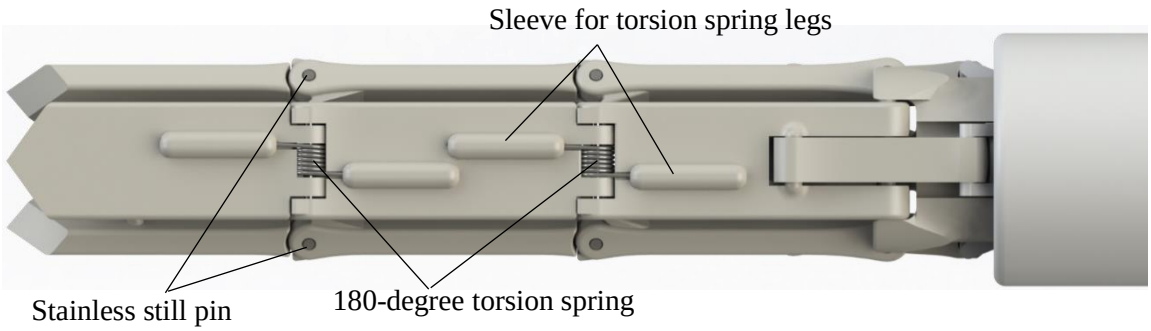

Fig. 28 Connection of the grasper's links

1mm stainless steel pins are used for joining links of the grasper finger together. 180-degree torsional stainless steel spring is used for keeping links two and three in a straight line with respect to link one.

Fig. 29 Full assembly of the middle tube and the three-fingered grasper

Proximal links, connecting links, slider ring, and middle tube are printed as a single interconnected part. Middle links and distal links are connected to the system separately.

Table 7. Technical Specs of the torsion springs used at joints of the grasper

Item	Material	Leg length (in)	Outside Diameter(in)	No. of coils	Wound Direction	Wire Diameter (in)	Torque @ ½ leg length(in.-Lbs.)
Torsion Spring	Music Wire	0.5	0.133	6.00	Left Hand	0.014	0.075

At distal end of the middle tube, a cubical space is designed for placement of the linear actuator of the forceps tube. Thus, when the middle tube is attached to the motor housing unit (MHU), the linear DC actuator with its leadscrew will be covered inside the housing of the middle tube. The middle tube is then fixed to the MHU using two stainless steel flathead screws.

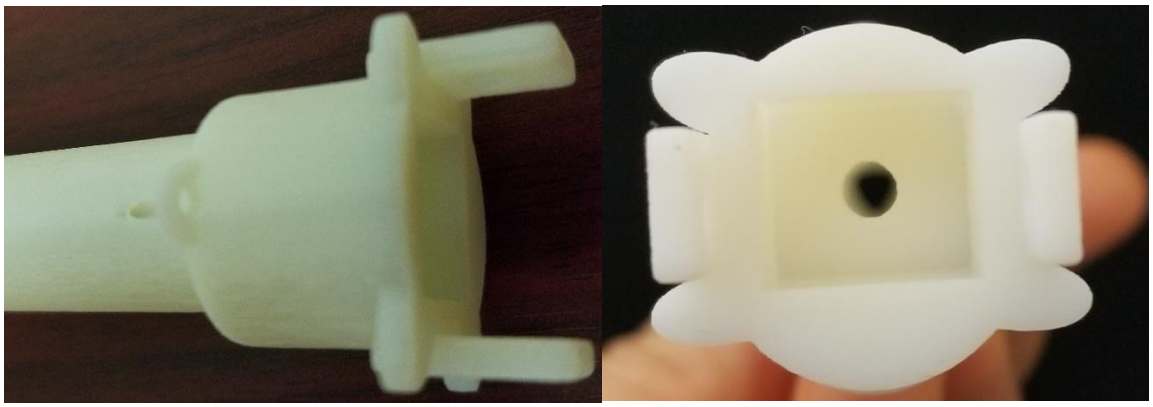

Fig. 30 Forceps tube's linear actuator housing block

The housing is located at the distal end of the middle tube. The hole at the surface of the middle tube in the left figure is for routing of the forceps cable. There is a similar whole at the other side of the middle tube, which is used for routing of the webbed three-fingered grasper's cable. The hole at the center of the linear actuator housing block in the figure on the right, is for the passage of the leadscrew of the linear actuator.

4.4 Grasping System

Although, the three-fingered grasper together with the specimen bag have the capability of encapsulation of the operative specimen, the grasper fails to effectively manipulate the excised specimen and retract it to its center. The reason is that, the grasper is designed as an underactuated mechanism with the aim of minimizing the number of actuators for the device. However, an

inherent issue with underactuated mechanisms is their limited manipulability. Hence, to account for this issue, a laparoscopic grasping forceps was adopted in order to compliment the function of the three-fingered grasper to carry out the manipulation and retraction stage of the specimen removal task.

4.4.1 MODIFIED ATRAUMATIC LAPAROSCOPIC GRASPING FORCEPS

A commercially available atraumatic fenestrated laparoscopic bowel grasping forceps (P216R, 5mm diameter, Aesculap Inc.) was purchased based on the requirements of the design table. After acquiring the instrument, its Jaw insert (P0770R, Aesculap Inc.) was decoupled from the rest of its components and was modified for use in RoboCatch. The stem of the jaw insert was cut approximately 5cm above the jaw mechanism. A 0.5 mm hole was drilled on the stem at 1mm distance from the cut end, for attachment of the actuation cable. A stainless steel disk with the diameter of 5mm and a hole at its center with the diameter of 1mm was inserted to the stem of the forceps and was fixed at a 3cm distance from the end of the cut. LOCTITE 2-part epoxy adhesive was used for fixation of the disk on the stem of the forceps. This disk functions as the platform where the compression spring exerts its force, pushing the disk forward to achieve the opening of the forceps jaws.

Fig. 31 Aesculap (P216R) laparoscopic grasping forceps (A) and its insert jaw (B)

Jaw insert was separated from the instrument to be modified for use in the RoboCatch. The red mark on the stem indicates the cutting point, which is approximately 5cm above the forceps jaws mechanism.

Additionally, a 3D-printed threaded insert (a 1cm long, M3× 5) was fitted to the head of the forceps for coupling it with the forceps tube. All components of the grasping forceps are shown in Fig. 32.

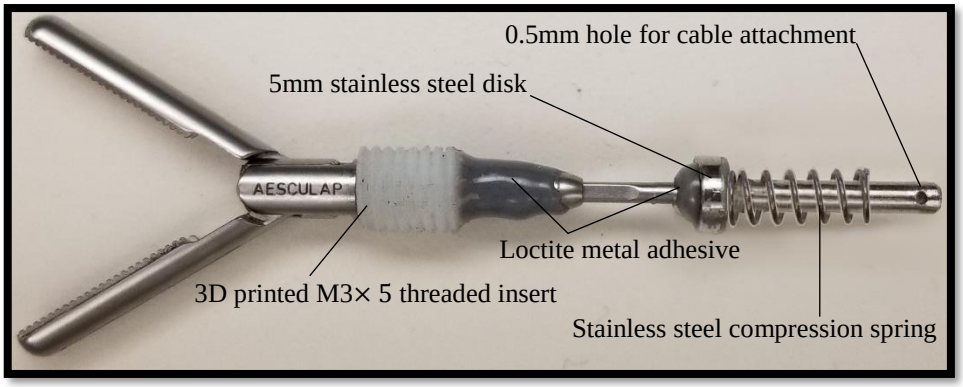

Fig. 32 Components of the modified grasping forceps of RoboCatch.

4.4.2 FORCEPS TUBE

The forceps tube is fabricated using the 3D printer. The forceps is fastened to a mating threaded cut (5×M3) at the tip of the forceps tube. When the forceps is fastened to the forceps tube, the compression spring will be arrested between two surfaces where one is fixed and the other one is moving resembling a cylinder-piston mechanism. The fixed surface is attached to the wall of the forceps tube with a 3mm hole at its center, which is used for the passage of the forceps cable. The moving surface is the fixed disk on the forceps that can move within the forceps tube like a piston in the cylinder-piston mechanism. When there is no tension on the forceps cable, the disk is pushed forward by the compression spring, resulting in the opening of the forceps jaws. When the motor pulls the cable, tension is produced on the cable, resulting in the closing of the forceps jaws. Fig. 33 shows the schematics of the opening and closing mechanism of the modified grasping forceps.

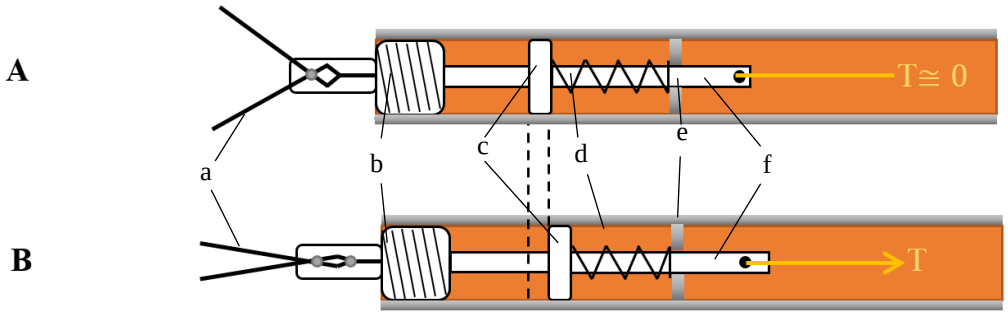

Fig. 33 Schematics of components of the grasping forceps used in RoboCatch

a) Grasper jaws, b) Threaded insert, c) Stainless steel disk, d) Compression spring, e) Fixed wall inside the forceps tube, f) forceps stem. A) Open state of the grasping forceps. When tension force of the cable is less than or equal to the compression spring force. B) Closed state of the grasper. When cable's tension force is more than the spring force.

The forceps cable runs through loops that are on the wall of the forceps tube and is attached to the end of the forceps stem. The axial translation of the tube is achieved by utilizing a DC motor with a leadscrew (M3× 5, 8cm long), which translates rotary motion into linear motion. Some advantages of the lead screw are its high load capacity, compact design with minimal number of parts, which makes it an ideal candidate for our application. The leadscrew is in a concentric position with the forceps tube, and is mated with a nut that is fixed at the end of the tube. The rotation of the leadscrew within the nut drives the forceps tube forward or backward, depending on the direction of rotation of the leadscrew. The maximum translation of the forceps is directly correlated with the length of the leadscrew. The leadscrew that was used in our device is 8cm long, which defines the maximum possible distance that the forceps can extend from its initial position. The translation speed of the tube has a direct relationship with the pitch of the leadscrew and the gearing of the DC motor. The smaller the pitch is or the higher the gearing ratio gets, results in a slower translation speed of the mechanism. The pitch of the lead screw was 0.5mm and the gearing of the DC motor was 100:1. Two grooves are created at the sides of the forceps tube that allows the tube to slide along the railings on the walls of the middle tube. These grooves eliminate the

torsional motion of the forceps tube and enable the linear movement of the tube along the leadscrew.

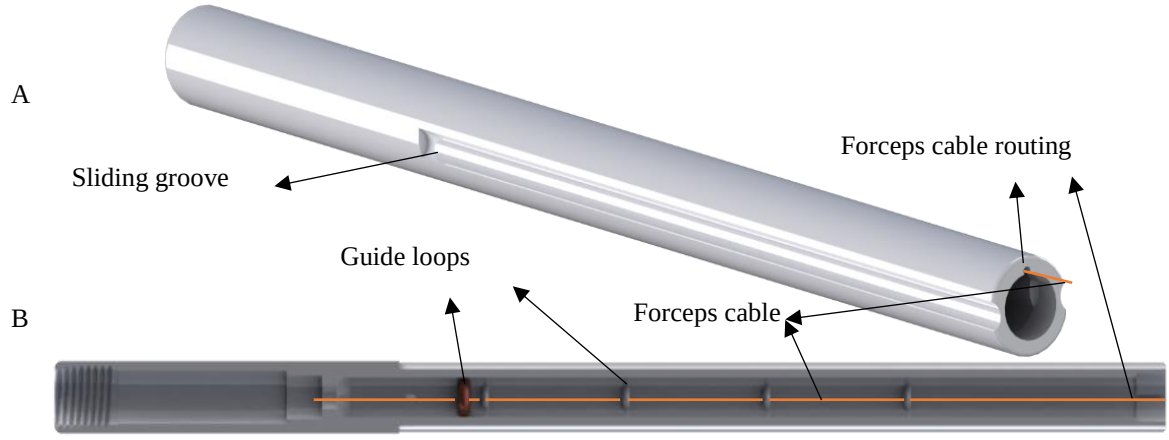

Fig. 34 Forceps tube

A) Grooves on the sides of the tube are for arresting the torsional motion of the tube and converting it to a linear motion. B) The sliced view of the inside of the forceps tube. Loops are placed at the side of the forceps tube to guide the cable to the stem of the forceps.

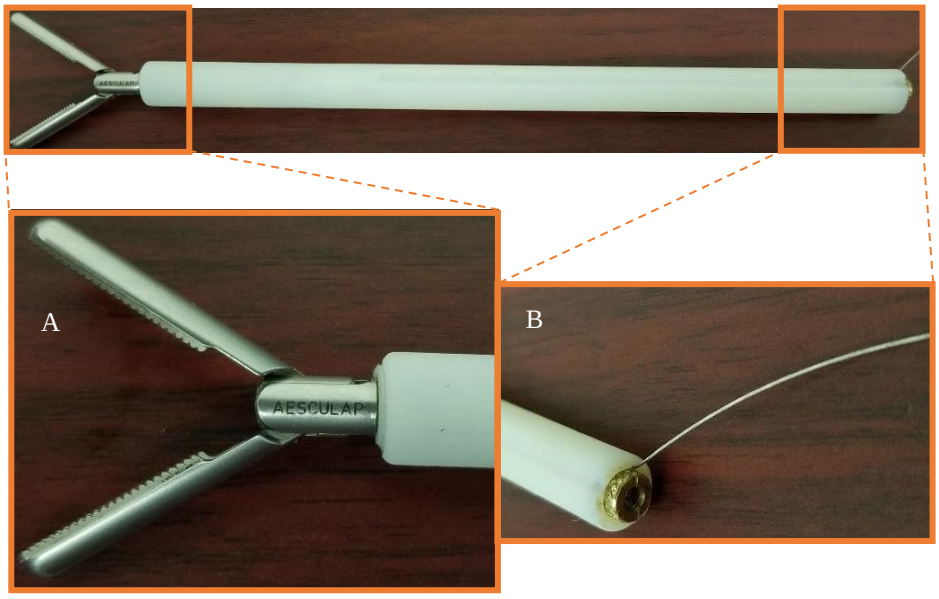

Fig. 35 Assembled grasping forceps system of RoboCatch

A) The Forceps is attached to the forceps tube by fastening the threaded insert on the forceps to the matching thread on the tip of the tube. B) The nut at the end of the forceps tube is mated with the leadscrew. The rotation of the leadscrew provides the linear movement of the system. The cable is passed through a small opening adjacent to the nut.

Table 8. Specifications of the compression spring used for the forceps mechanism

Item	Material	Leg length (in)	Outside Diameter(in)	Compressed Length(in)	Spring Rate (lb./in.)	Wire Diameter (in)
Compression Spring	Stainless Steel	0.5	0.18	0.176	8	0.020

4.5 Motor Housing Unit (MHU)

There are three brushed geared DC motors placed inside this unit. One motor is responsible for closing of the grasping forceps, the other one is responsible for closing of the fingers and specimen bag, and the third motor has a built-in leadscrew at its output shaft that provides the axial movement for the grasping forceps. Four V groove ball bearing roller guides, two at each side of the MHU, are used for facilitating the sliding motion of MHU inside the linear rail of the main tube frame. An annular Snap joint is used for attachment of the V groove guide bearings to the MHU. This design obviates the need for using fasteners for connecting the guide roller to the MHU, therefore, reducing the risk of loose connections in the device and easier maintenance of the system.

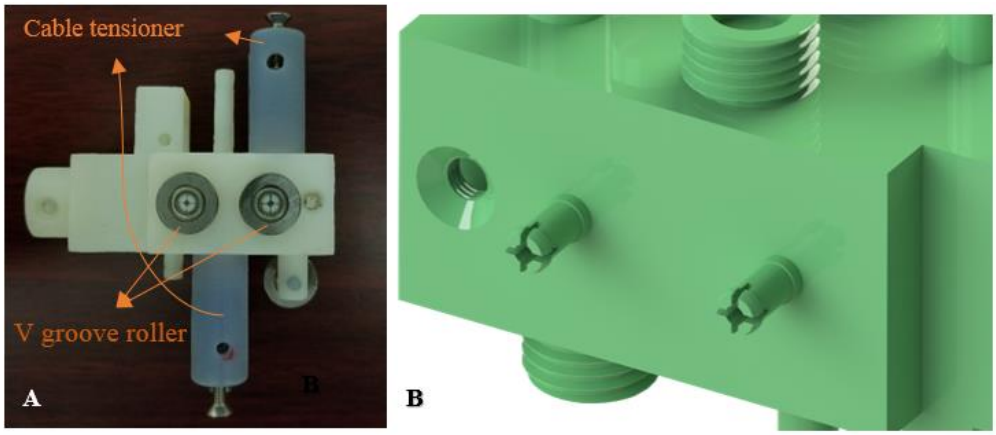

Fig. 36 Motor Housing Unit (MHU)

A) MHU with V groove roller guides. Tensioners are used at the top and bottom of the MHU to maintain essential tension in the cables. B) A close-up view of the annular snap joint. The diameter of the joint at its tip is slightly more than the inner diameter of the V groove roller. Thus, when the pulley is inserted inside the joint, the tip of the joint is deflected and allows the roller to be inserted. After the insertion, the tip will go back to its initial diameter thus keeping the roller secured at its position.

At the back of the unit, the linear servo actuator is connected to the MHU via a pin. Two DC motors that are responsible for closing of the Fingers and closing of the grasping forceps are placed in the opposite orientation with respect to each other, with one of them facing up and the other facing down. The motor at the top, is used for the closing of the grasping forceps and the motor at the bottom, is used for closing of the fingers of the grasper and closing the opening of specimen bag. Both motors are fixed at their position by two M1.6 screws that attach each motor to the MHU. The third motor is placed at the front of the unit. This motor is a brushed geared DC motor with a lead screw that is responsible for providing linear actuation for the grasping forceps. The motor is covered and secured at its position by the middle tube.

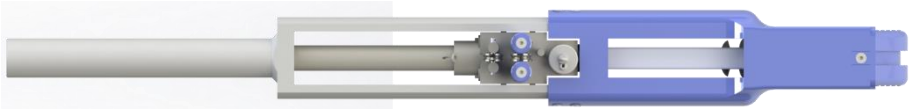

Fig. 37 Top view of the RoboCatch

Middle tube is attached to the front of the motor housing unit. In this figure, the linear servomotor, which is responsible for the movement of the MHU, is fully retracted, thus, setting the MHU to its initial position with all instruments retracted inside the main tube.

4.6 Tensioner

Tensioners are crucial components in cable-actuated mechanisms, where they are used for maintaining the essential tension in the cables. There are two cable driven mechanisms in our device; one is for the opening and closing of the grasping forceps and the other one is for the closure of the fingered grasper and the specimen bag. The tensioner that we developed for our device resembles a piston-cylinder mechanism. Tensioners consists of two cylindrical poles with compression springs placed inside each of them. A smaller diameter cylindrical component is placed within each pole and on top of the compression spring. The smaller component can freely

move up and down within the cylinder. However, the downward movement of the smaller cylinder is resisted by the compression spring. Smaller cylinders at each pole are attached to each other via a pin. Thus, the movement of both components are similar. A V groove roller guide similar to the one that is used for the linear movement of the MHU, is inserted into the connecting pins and is fixed between the two poles. Cable is wound around the roller guide, and then, it is passed through a fixed hole on a pole on the MHU, and finally, is attached to the pulley on the motor. The fixed holes have the duty to level the cables with the motor pulley before they are attached to the motor. This eliminates the sliding of the cables out of the motor pulley and helps with a uniform winding of the cable around the motor pulley. The cable pulls the pulley down resulting in the compression of the springs inside the tensioner. While operating the device, once the tension inside the cable is decreased, the compressed springs in the tensioner push the v groove pulley upward, hence, maintaining the essential tension in the cable.

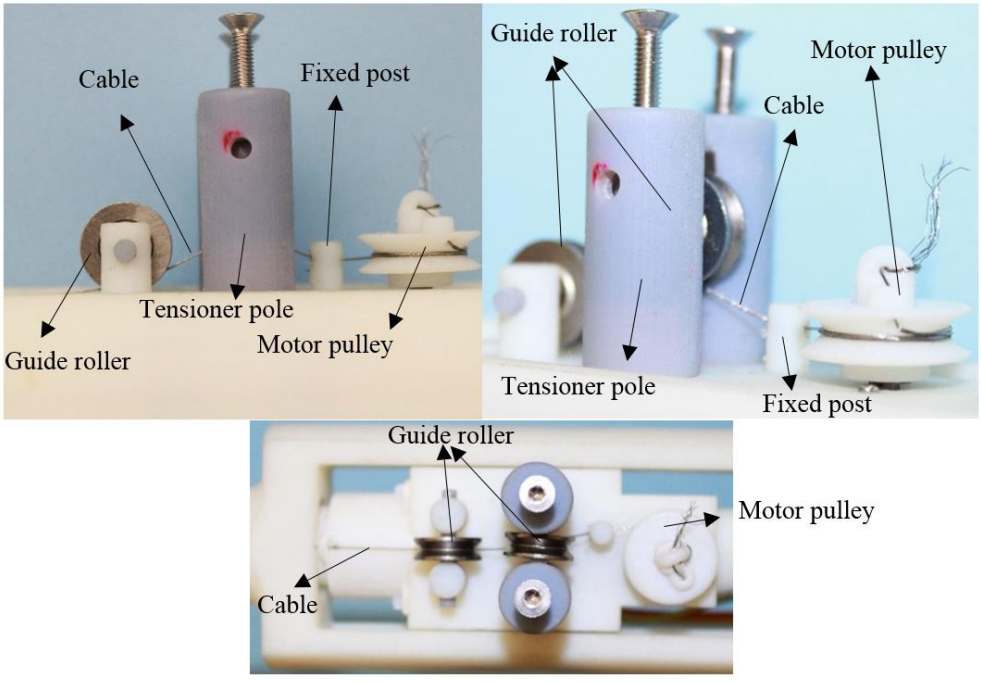

Fig. 38 Tensioner mechanism of the grasping forceps cable

Motor and the tensioners of the grasping forceps are positioned on the top of the MUH.

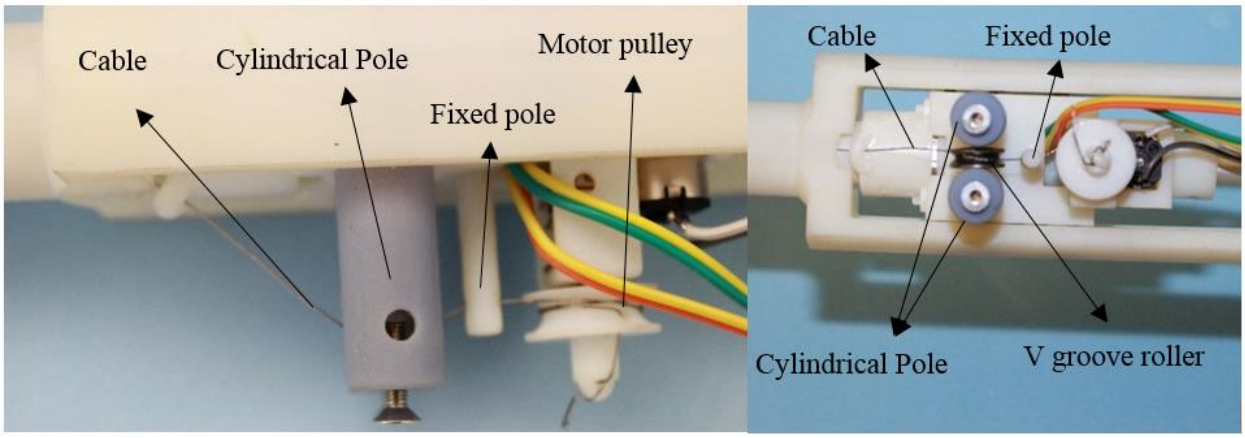

Fig. 39 Tensioner mechanism of the fingered grasper cable

Motor and tensioner for the closing of the fingered grasper are positioned on the bottom of the MUH

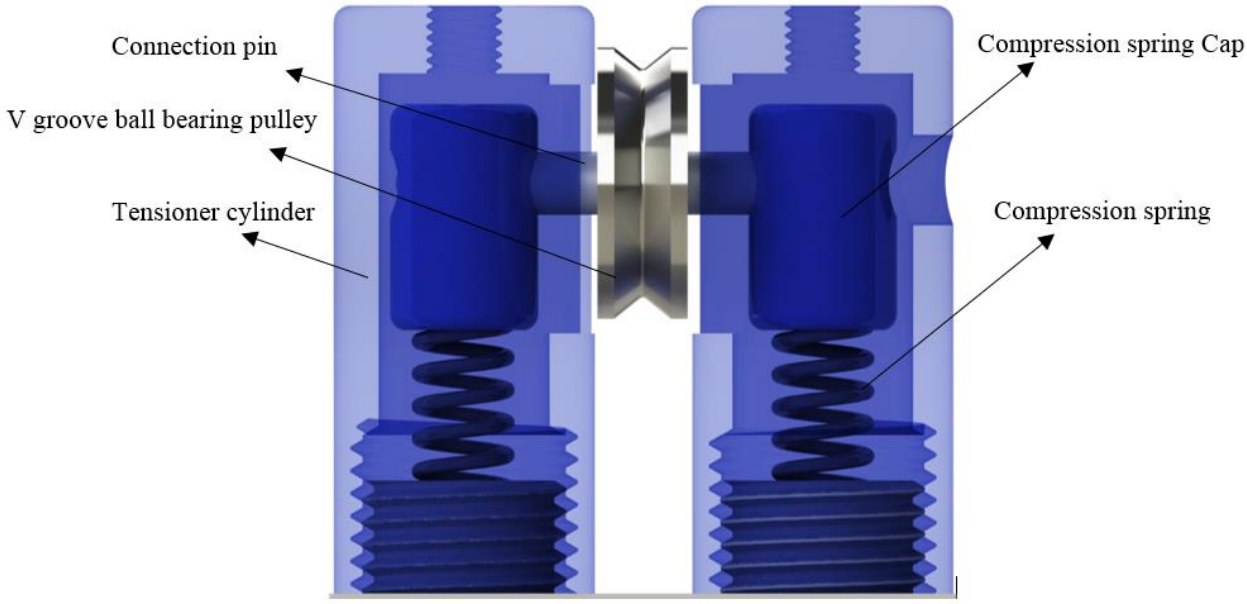

Fig. 40 CAD model of tensioner and components inside

Table 9. Specifications of the compression spring used in tensioner

Item	Material	Leg length (in)	Outside Diameter(in)	Compressed Length(in)	Spring Rate (lb./in.)	Wire Diameter (in)
Compression Spring	Stainless Steel	0.5	0.18	0.144	6	0.018

4.7 Actuator and Control Units

Four motors are responsible for the actuation of our robot. The first motor is a micro linear DC servomotor (L12-R manufactured by Actuanix®) that is connected to the MHU. Since MHU is directly connected to the middle tube and the forceps tube, the linear movement of MHU will also results in the linear motion of the forceps and grasper. Hence, the actuation of this motor leads to the deployment of the webbed three-fingered grasper unit out of the main tube. This marks the first stage of the specimen retrieval task of the RoboCatch. Two benefits of using servomotors are their high accuracy of movement and their ability to be controlled using position control. The input to this motor is in terms of numerical position values that are given by the surgeon using the joystick controller. Thus, the motor's movement is based on the direction of the deflection of the joystick handle, where the downward deflection of the joystick drives the motor forward and the upward deflection of the joystick retracts the motor. After receiving the position command, the motor will go to the exact position as commanded. Once it reaches there, it will hold its position and waits for the next position command. Fig. 41 depicts the micro linear actuator used in the RoboCatch. Additionally, Table 10 provides the specifications of the linear servomotor.

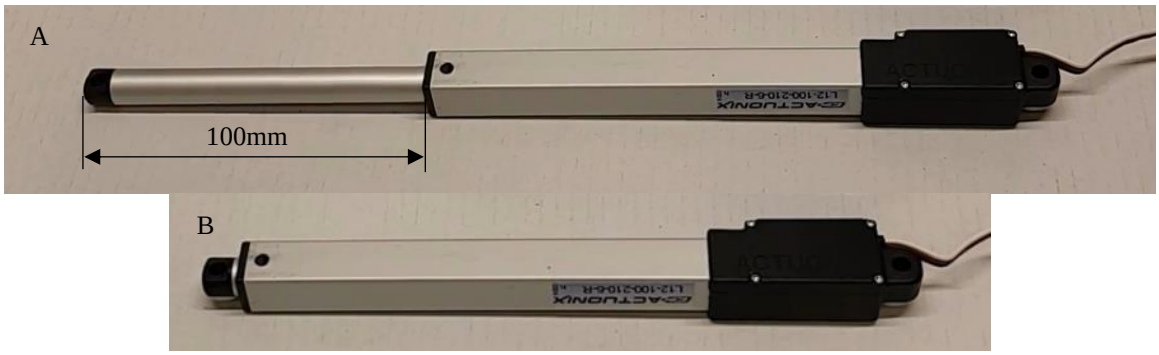

Fig. 41 Linear micro servomotor (L12-R manufactured by Actuanix®)

A) Motor is at its fully extended state. A cylindrical rod extends out of the motor providing the axial motion. B) Motor at its fully retracted state.

Table 10. Technical specifications of the linear servo actuator L12-R

Gearing option	100:1
Peak Power Point	17N @ 10mm/s
Dimensions	152mm×15.1mm ×18mm
Max Speed	6.5 mm/s
Max Force	80 N
Back Drive Force	45 N
Mass	56 g
Repeatability	±0.5 mm
Closed length	152 mm
Voltage	6V
Stroke Length	100 mm

As described in section 4.5, all motors other than the linear servomotor are housed within the MHU. All of these motors are geared brushed micro DC motors; however, they have different gearing and output shaft configurations. One DC motor is responsible for actuation of the grasping forceps. This motor is placed at an upright position inside the MHU. The output shaft of the motor is attached to a 3D printed pulley. This pulley is connected to a cable that is attached to the forceps mechanism and is used for closing action of the forceps. For closing of the forceps, the cable needs to be wound around the pulley. Deflection direction of the joystick controller determines the rotation direction of the motors. Clockwise (CW) motion results in the closing of the forceps and the counter-clockwise (CCW) rotation results in the opening of the grasping forceps.

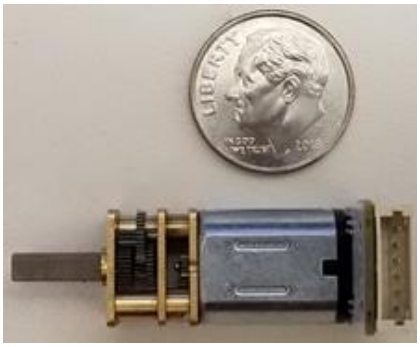

Fig. 42 Brushed micro DC gear motor

These motors offer high torque in a compact size, which makes them ideal for use in our device. These motors are used for closing of the grasping forceps and the webbed three-fingered grasper.

Another motor with similar specifications is used for closing of the webbed three-fingered grasper. This motor is positioned in front of the forceps motor in an upside down orientation. The reason for this placement arises from the presence of extreme space constraints. If we had opted to place both motors in front of each other with the same orientation, the pulley of each motor would collide with each other; therefore, we had two options for solving that issue. Either we could increase the distance between the two motors, or we could place them at an opposite orientation with respect to each other. The issue with the first solution is that by increasing the distance between the two motors, the overall size of the MHU would have increased. This could have led to a bulky design of the device that was in conflict with the design criteria of our device. For this motor, the closing of the fingered grasper and the specimen bag is achieved by the CW rotation of the motor shaft.

The third motor on the MHU is a DC motor with the leadscrew that provides the linear motion of the grasping forceps. A matching nut is inserted into the end of the forceps tube and is mated with the leadscrew of the DC motor. The rotational movement of the forceps tube is constrained inside the middle tube. Thus, when the leadscrew rotates, the rotational movement is translated into the linear movement of the forceps tube. The CW rotation of the motor drives the forceps forward and the CCW rotation of the motor reverses the movement of the forceps. Table 11 provides technical specifications of the DC motors used in the RoboCatch.

Table 11. Technical specifications of the micro brushed DC gear motor

Gear Ratio	297.92:1
No Load RPM	100
Stall Current	1.6A
Rated Torque	15.4 oz.-in
Stall Torque	70 oz.-in
Shaft Type	D-Shaped
Dimensions	10H×12W×26L mm
Weight	9.5 g
Voltage	6V

Fig. 43 Brushed micro DC gear motor with lead screw

Table 12. Technical specifications of the micro brushed DC gear motor with leadscrew

Gear Ratio	100:1
No Load RPM	155
Instant Torque	1.5 kg.cm
Rated Torque	0.7 kg.cm
Shaft Type	M3× 5 Leadscrew
Dimensions	10H×12W×110L mm
Weight	24 g
Voltage	6V

As mentioned earlier, control of all actuators of the RoboCatch, is achieved by utilizing an onboard dual-axis joystick controller. This controller transmits the analog signals of two potentiometers of each joystick axis to a microcontroller unit (Arduino Mega 2560 R3). The microcontroller reads the analog values and runs them inside the control program of the robot where the analog values are mapped to motor speed values. Afterwards, output signals are sent to DC motor driver (L298H) that is in charge for pulse width modulation, and from there, generated pulses are sent to the actuators to provide them with the required voltage for achieving the desired movement. The joystick used has only two outputs and a switch button. The outputs are x-axis and y-axis outputs. Two different outputs means that the joystick can give inputs to up to two actuators at any given time. This presents a challenge in controlling our device, which has more than two actuators. To address this issue, we divided the robot's task of specimen retrieval into three stages.

These stages are defined as the following: 1) Deployment of the fingered grasper, 2) retraction of the specimen, 3) containment of the specimen.

In each stage, only up to two actuators are used for the execution of that task. Benefiting from this, we came up with a control scheme that defines three different control modes for the joystick that correspond to each stage of the task. In each mode, the joystick would actuate certain motors and the operator chooses between the modes by pressing down on the joystick. Each press would change the mode to the next one. For instance, if the joystick was in mode one, one press on the joystick would change the setting to mode two. Mode one was allocated to the first stage of the retrieval task, where only linear servomotor is utilized. In this stage, pushing down on the joystick would drive the motor forward, which results in the deployment of the fingered grasper outside of the main tube of the device. In mode two, the joystick controls the linear movement, opening, and closing of the grasping forceps. The up and down deflection of the joystick in this set results in the extension and retraction of the forceps respectively. Deflection of the joystick to the left closes the jaws of the forceps and the deflection to the right opens the jaws. Finally, in the third mode, the only actuated motor is the one that is responsible for the closure of the fingered grasper and tightening of the specimen bag, where pushing the joystick up tightens the bag and closes the fingered grasper. Fig. 45- Fig. 47 demonstrate various control stages of the RoboCatch.

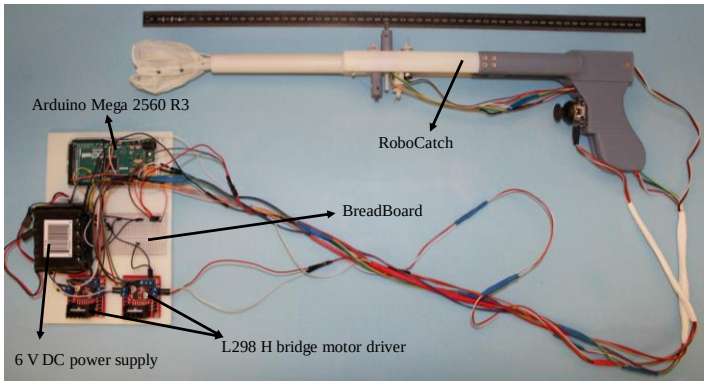

Fig. 44 Control units of the RoboCatch

Mode 1

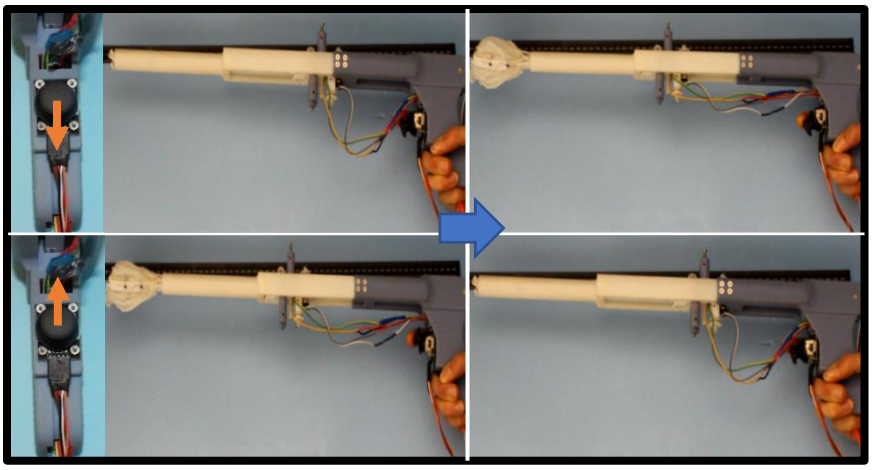

Fig. 45 Control of the RoboCatch in mode one

In mode one, pushing the joystick up deploys the fingered grasper out of the main tube and pushing the joystick down will retract the fingered grasper inside the main tube.

Mode 2

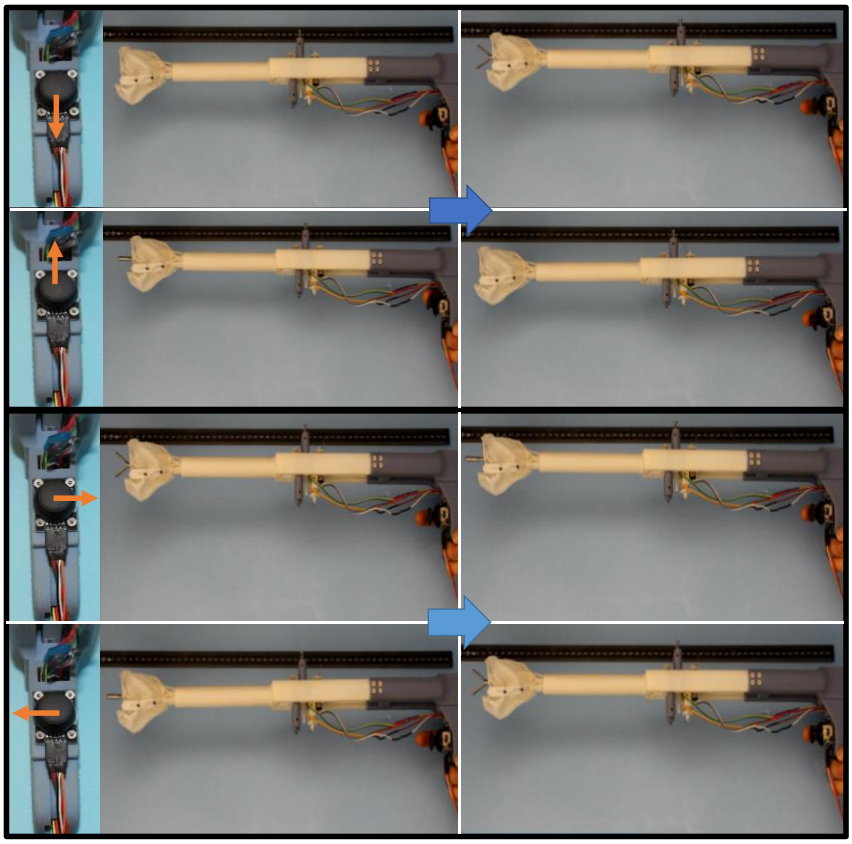

Fig. 46 Control of the RoboCatch in the mode two

In mode two, pushing the joystick to the right closes the forceps, while pushing the joystick left opens forceps jaws. The forward movement of the forceps is achieved when the joystick is pushed down, and the retraction inside the base is commanded with the upward deflection of the joystick.

Mode 3

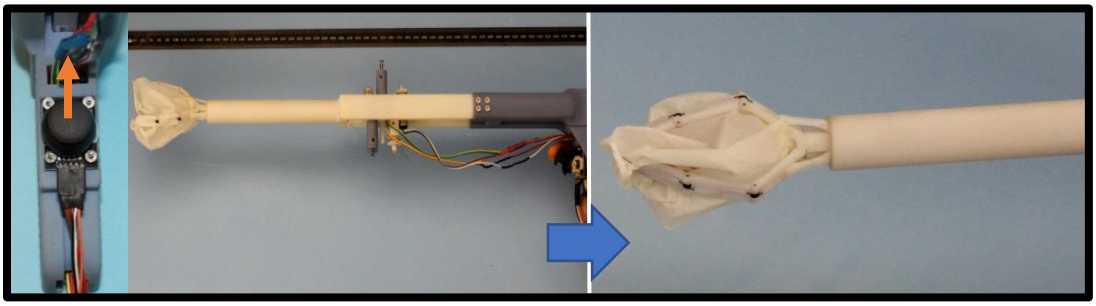

Fig. 47 Control of the RoboCatch in mode three

Closure of the bag and fingered grasper is achieved by deflecting the joystick handle upward.

CHAPTER 5

5 EXPERIMENTAL VALIDATION

Initially, the working of each mechanism of the device including the webbed three-fingered grasper and the grasping forceps was tested to investigate the desired functionality of those mechanisms. During those tests, several aspects of various parts including the grasping force of the forceps, routing of the cables, linear movement of the forceps tube, and closing of the fingered grasper were investigated. Several design iteration had to be made until a well-working prototype was achieved. Later, porcine meat sample was used to examine the capability of the Robocatch in the specimen retrieval task inside a simulated laparoscopic trainer box. These tests were conducted to evaluate the range of masses and topologies of specimens that the Robocatch can successfully retrieve and encapsulate. These tests demonstrated that the Robocatch is capable of retrieving specimens with masses ranging from 1-50 grams. Additionally, the robot was able to successfully engulf specimens ranging from 1-40 grams in mass and volumes ranging from 1.53 - 75.46 milliliters.

5.1 Characterization Experiments

The initial experiment was conducted to characterize the capabilities of the Robocatch regarding the range of the masses of the specimens that it can successfully grasp and retract. Additionally, we were interested in determining the maximum volume of the specimens that the Robocatch could fully contain within its fingered grasper. We chose to use porcine meat as our phantom specimen because of its close similarities with human tissue. We purchased porcine meat from a local general store (Food lion, Norfolk, VA 23508). Porcine meat sample was then cut into various sizes with masses ranging from 1-100 gram. After weighing all of the specimens, the dimensions of each specimen were collected. All measurements for each specimen can be found

in Table 13. Fig. 48 shows porcine meat samples that were used in the characterization experiment. Each sample was put on top of the experiment table, where an operator performed the task of specimen retrieval using the Robocatch.

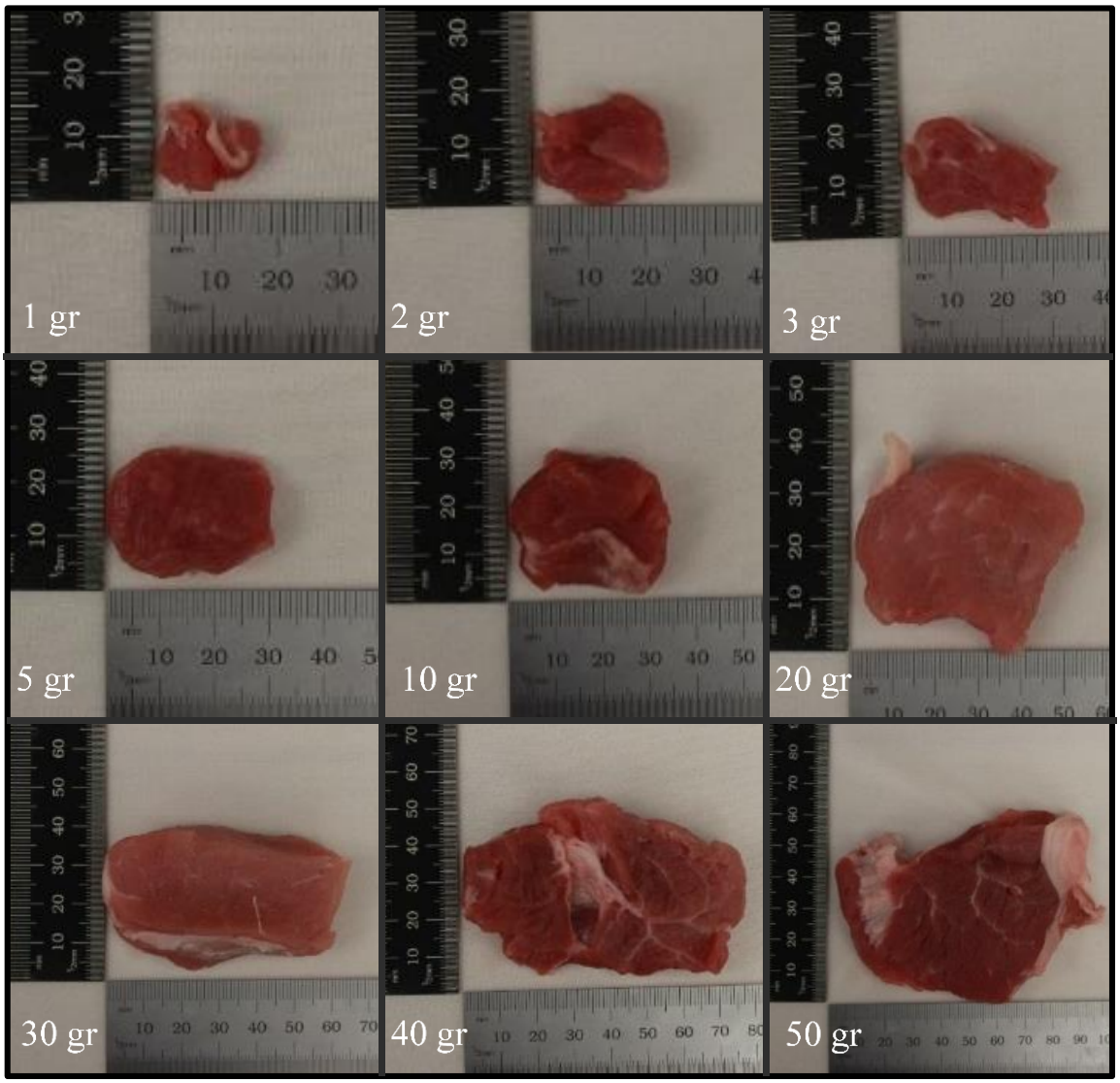

Fig. 48 Porcine meat samples

The smallest specimen had a mass of 1 gram, whereas, the largest specimen that the grasping forceps could successfully grasp and retract was 50gr. Although the grasper could grasp and retract the 50gr specimen, however, it failed to successfully place it inside the fingered grasper. The reason was that the volume of the 50 gr specimen was greater than the enclosed volume of the fingered grasper.

Table 13. Measurements of the porcine meat samples used in the characterization experiment

Weight (gr)	Length (mm)	Width (mm)	Height (mm)	Volume (ml)
1	17	15	6	1.53
2	24	18	10	6.48
3	30	23	10	6.9
5	31	26	13	10.478
10	35	32	14	15.68
20	54	37	15	29.970
30	66	37	17	41.514
40	77	49	20	75.46
50	91	62	17	95.914

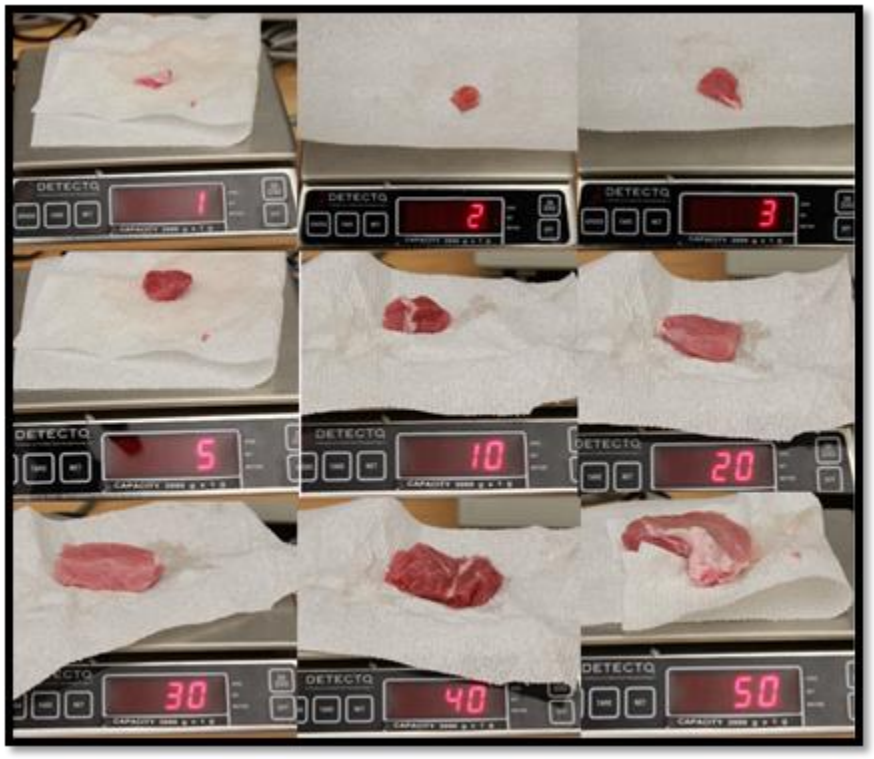

Fig. 49 Weighing of porcine meat samples

A scale with an accuracy of $\pm$ 1 gr (Detecto AP-4K) was used to cut each specimen to exact desired masses.

We started the test with the smallest sized specimen. We would proceed to the next larger specimen only if the trial on the current specimen was executed successfully. Thus, the experiment stops at the largest specimen that the robot could successfully grasp, retract, and engulf. In each trial, the RoboCatch was set to its initial configuration, which is to retract all of its instruments inside its main tube. Afterwards, the robot was handed to an operator to execute the specimen retrieval task. Samples were placed in an open surface, where the operator could have a direct visual of the specimen and then the retrieval task was initiated. We consider a trial successful, when the specimen is grasped securely and is retracted to the center of the webbed three-fingered grasper without falling off the grasping forceps. We were also careful that the retracted specimen was fully placed inside the fingered grasper and no portion of it is remained outside, when the specimen is engulfed by the grasper. We tested the total of nine specimens ranging from 1 to 50 grams. Eight of these specimens were successfully grasped and retracted to the fingered grasper and contained within the webbed grasper. However, the 50 gr specimen could not be inserted inside the webbed grasper. The reason was that the dimensions of the specimen exceeded the volume of the webbed grasper. Fig. 50 demonstrates the full phase of the specimen retrieval task of the RoboCatch. These phases involve: 1) deployment of the webbed-three fingered grasper, 2) extension of the grasping forceps out of the middle tube toward the specimen, 3) grasping of the specimen, 4) retraction and placement of the specimen inside the webbed three-fingered grasper 5) Engulfment of the specimen by the three-fingered grasper. Additionally, Fig. 52 demonstrates grasping, retraction, and placement stage of the specimen retrieval task for all nine specimens.

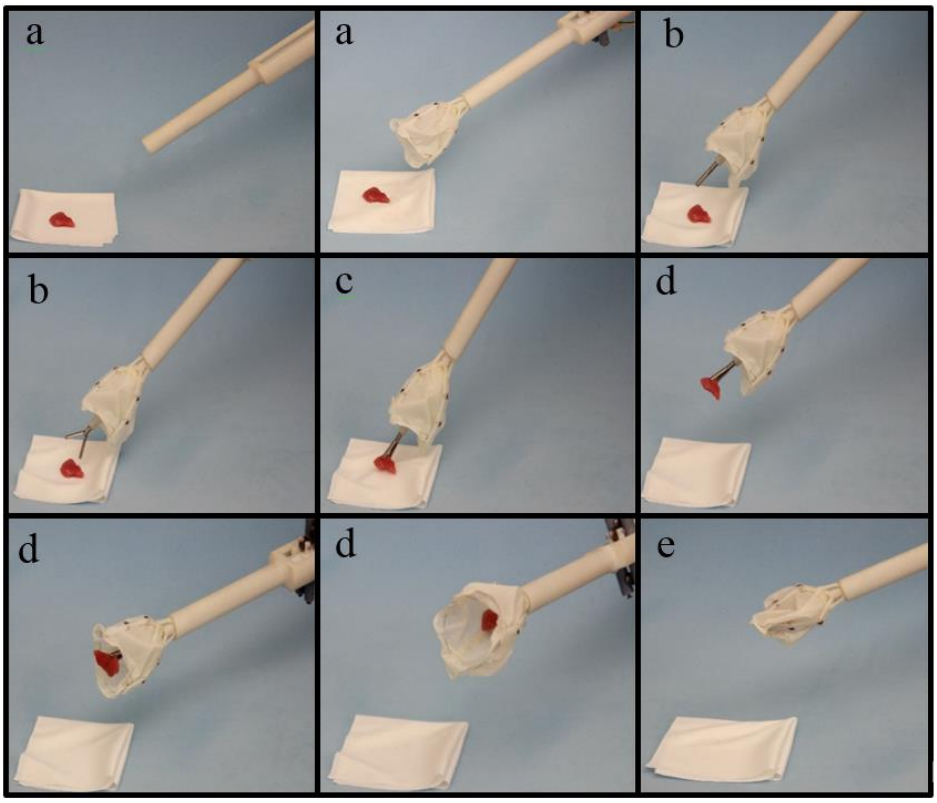

Fig. 50 Full phase of specimen retrieval operation of RoboCatch in an open environment

The specimen tested is a 5 gr porcine meat sample. a) Deployment of the webbed-three fingered grasper, b) Extension of the grasping forceps out of the middle tube toward the specimen, c) Grasping of the specimen, d) Retraction and placement of the specimen inside the webbed three-fingered grasper, e) Engulfment of the specimen by the three-fingered grasper.

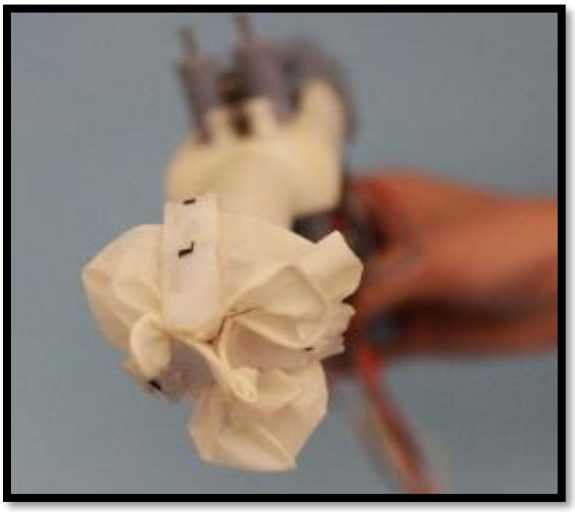

Fig. 51 Robocatch engulfing the retrieved specimen

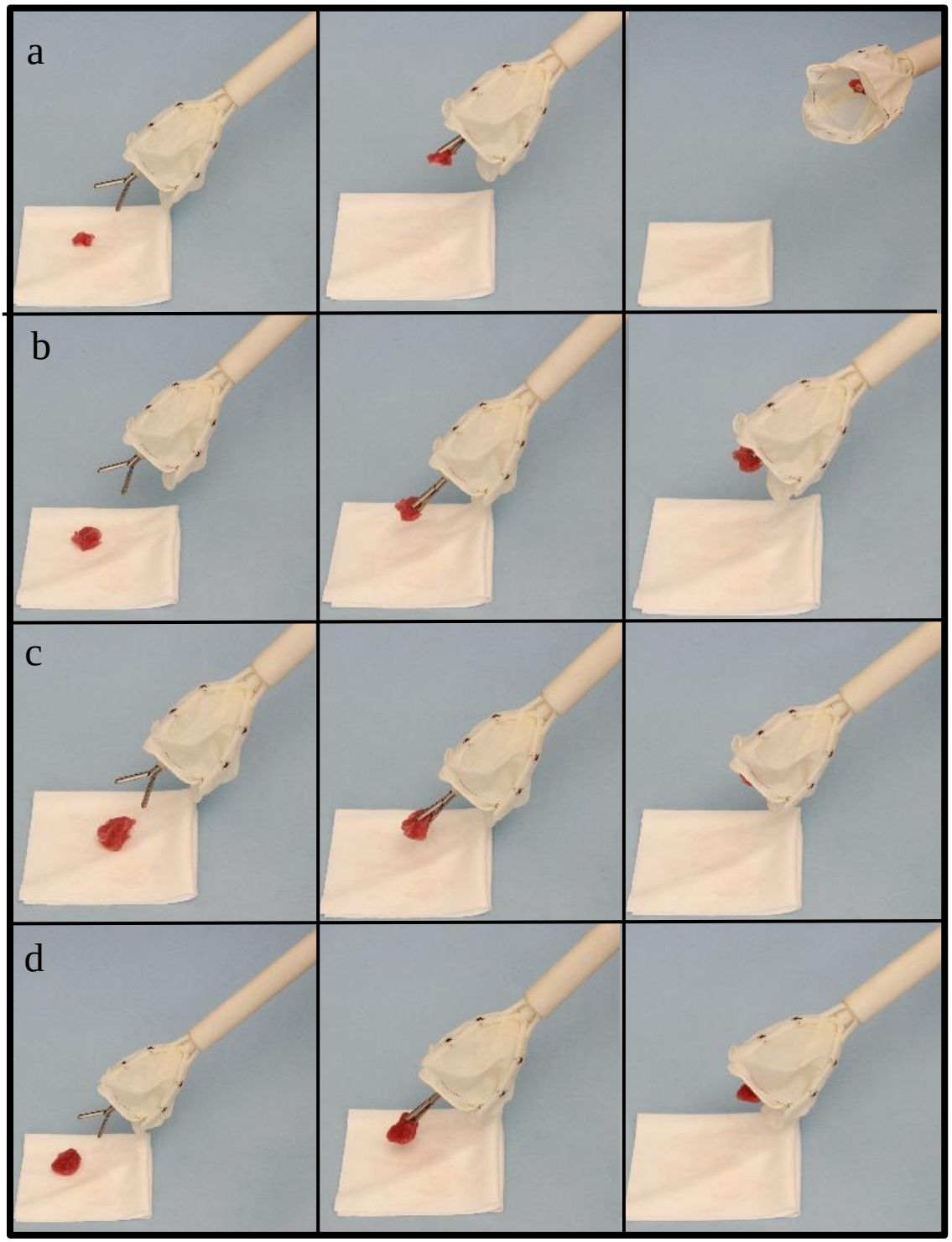

Fig. 52 Grasping, retraction, and placement stages of the specimen retrieval by the RoboCatch

a) 1gr specimen, b) 2gr specimen, c) 3 gr specimen, d) 5 gr specimen, e) 10 gr specimen, f) 20gr specimen, g) 30 gr specimen, h) 40 gr specimen, i) 50 gr specimen.

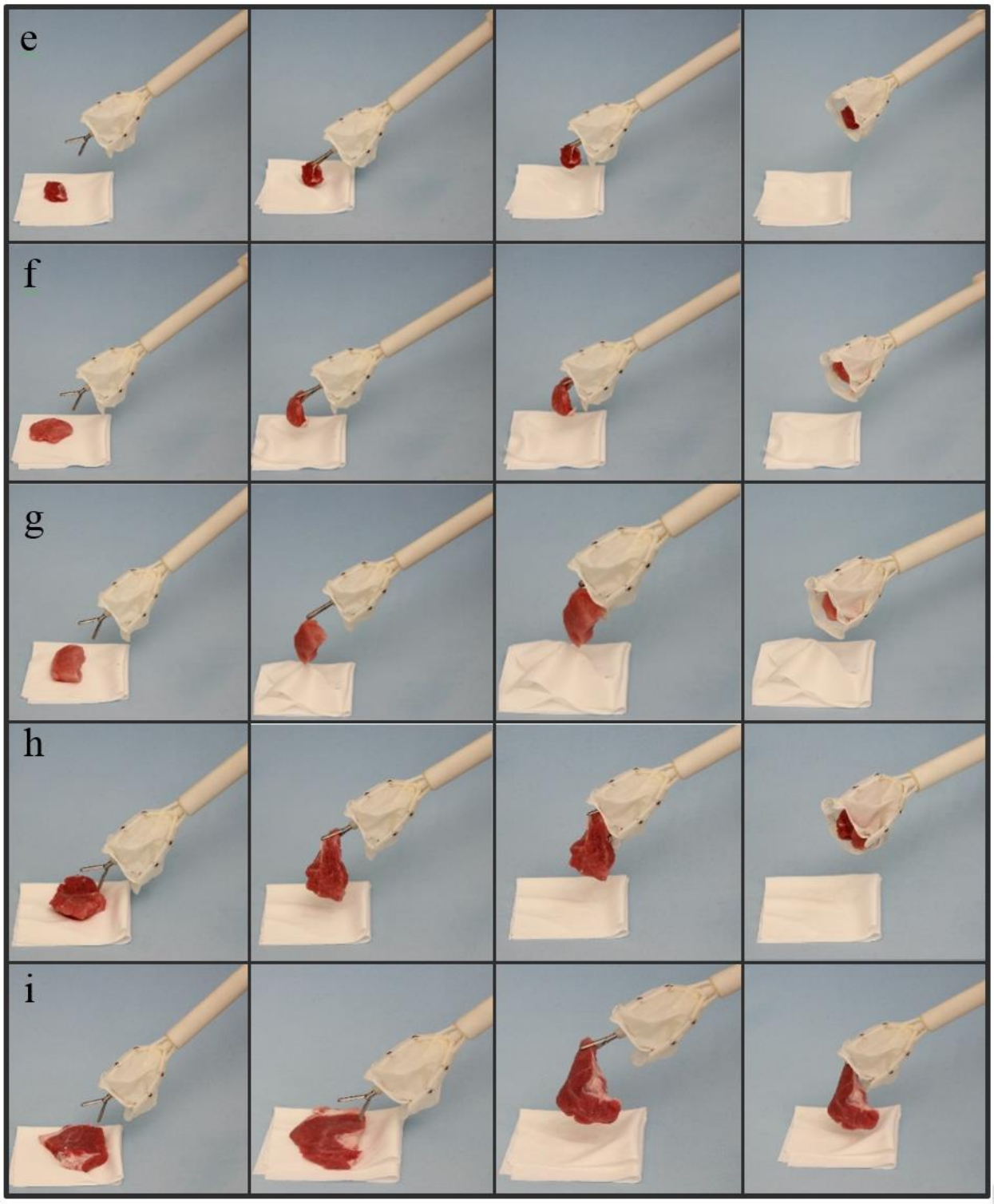

Fig. 52 Continued

5.2 Specimen Retrieval in a Simulated Environment

A laparoscopic trainer box was built using a clear plastic storage box (Rubbermaid®) with dimensions of 13L×8W×5H inches. The lid of the trainer box was covered so that it would obscure the direct view of the operator to the specimen inside the box. Two holes are created on the lid; one is for the insertion of the Robocatch and the other one is for the visualization of the interior of the trainer box using a camera. Visual images of the camera are displayed on a monitor that is in front of the operator and are used as visual feedbacks to the operator to locate and track the position of the specimen inside the box while operating the RoboCatch. Another camera is put in front of the trainer box, which is used for recording the processes from a different view. The robot was set to its initial position before the start of the experiment. The operator then started the procedure by inserting the main tube through the hole on the top of the trainer box. The webbed three-fingered grasper was successfully deployed inside of the trainer box. After locating the specimen using the visual images on the monitor in front of the operator, the forceps tube was extended towards the specimen. After a few attempts, the grasping forceps successfully grasped the specimen. In the next stage, the operator retracted the specimen to the center of the webbed three-fingered grasper. Finally, the fingered grasper was closed on the specimen and the specimen bags opening was tightly closed.

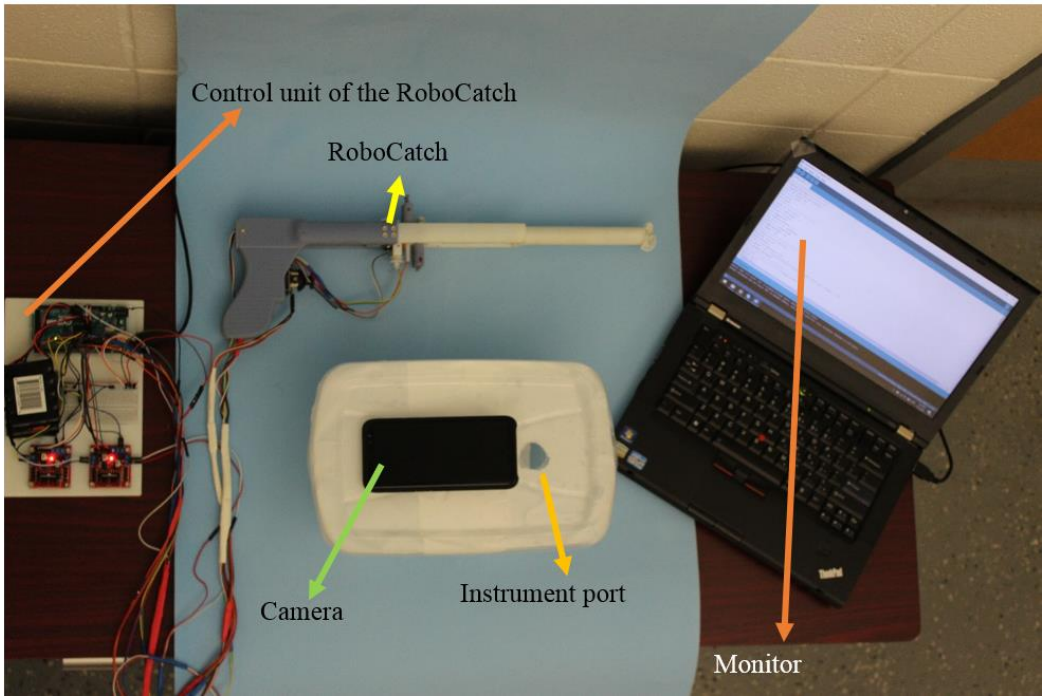

Fig. 53 The experimental setup for the specimen retrieval using trainer box

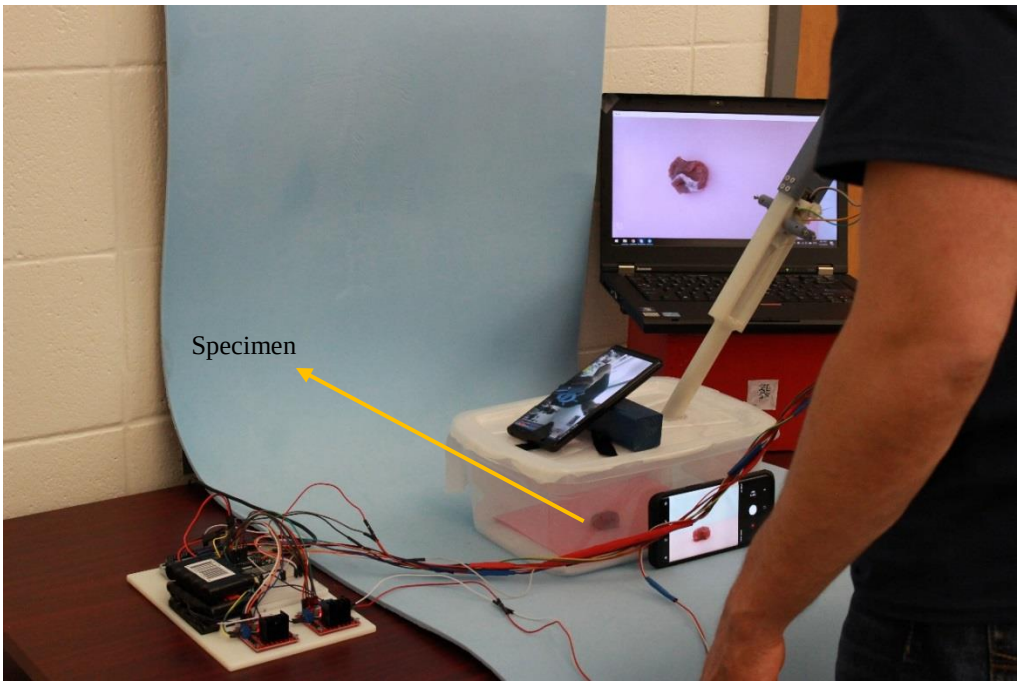

Fig. 54 Retrieval of the specimen inside the box trainer by an operator

The camera on the top of the box trainer provides the visualization of the inside of the box. The images are displayed on the monitor in front of the operator.

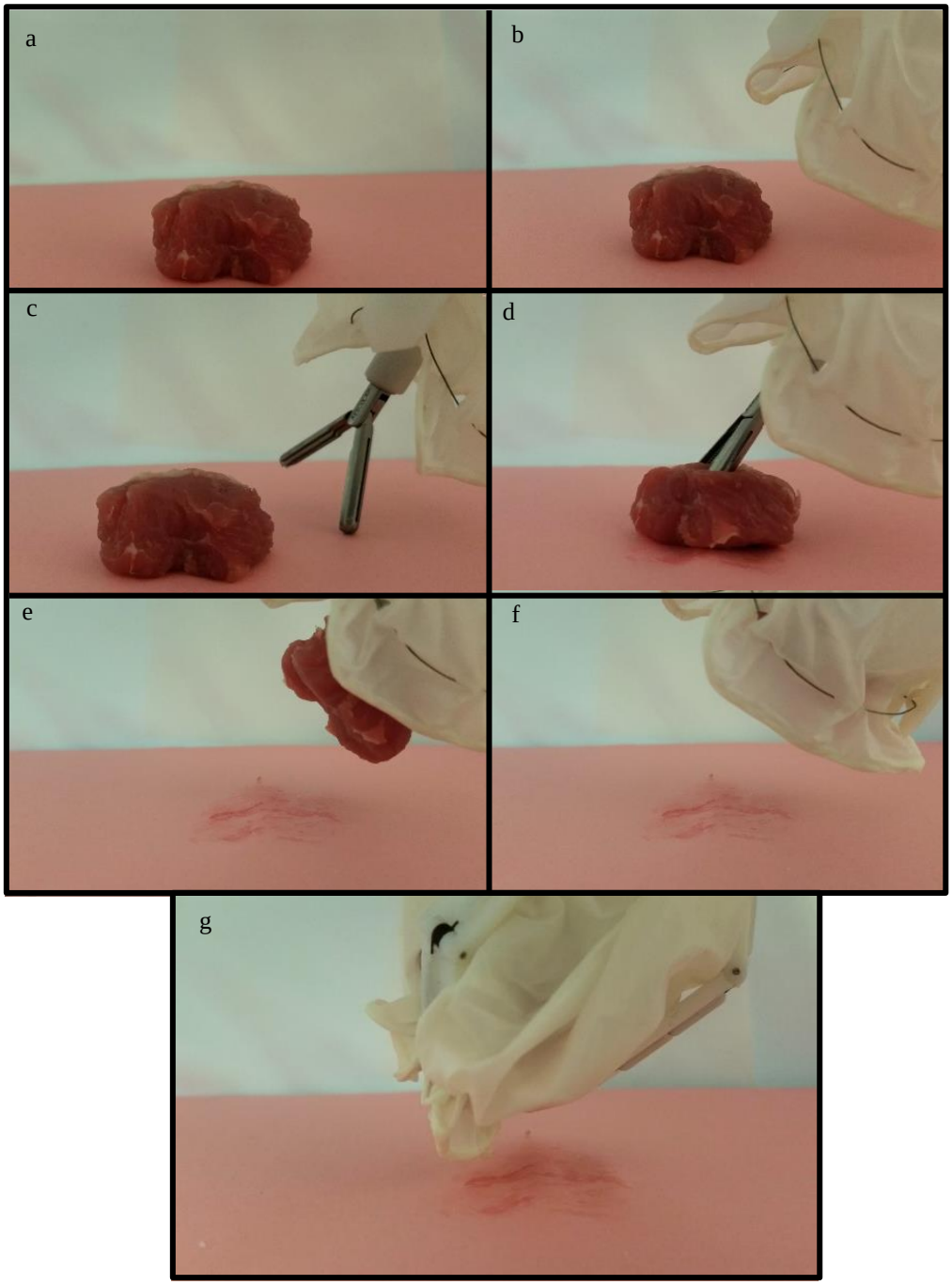

Fig. 55 Inside view of the of the trainer box capturing specimen retrieval stages

a) The 10 gr porcine meat sample is placed inside the trainer box, b) Webbed-three fingered grasper is deployed, c) Grasping forceps are extended out of the middle tube toward the specimen, d) The specimen is grasped, e) The specimen is retracted, f) The specimen is placed at the center of the webbed three-fingered grasper, e) The specimen is fully contained by the webbed three-fingered grasper.

CHAPTER 6

6 CONCLUSIONS AND FUTURE WORK

This thesis involved the design and making of RoboCatch, a novel hand-held robot for the task of spillage-free retrieval of operative specimens, typically performed after their resection during laparoscopic surgery, with applications in fields ranging from gynecology to oncology. The design of the device was based on the requirements of the surgeons in the field for a portable hand-held device that would minimize the number of active ports required for contained extraction of specimens, while offering an intuitive control of the system. This was achieved in the proposed design by significantly modifying and extending conventional instruments that are currently used by surgeons for the retrieval task. A distinguishing feature of RoboCatch is the webbed three-fingered grasper that avoids any spillage of the specimen during retrieval. The atraumatic forceps used to pull the specimen into the center of the grasper facilitates a relatively easier engulfing of the specimen by the grasper and obviating the need for use of an additional instrument for grasping and placement of the specimen inside the specimen bag. The design benefited from a minimal number of actuation units that lowers the cost of fabrication of the instrument and allows for a simple control scheme. The device was fabricated using an Object Prime 3D printer and was tested for its practical application. Various capabilities of the device such as the maximum grasping force and the maximum volume of a specimen that the robot can retrieve were investigated through the experiments. Specimen retrieval experiments were conducted with porcine meat samples to test the feasibility of the proposed design. Experimental results revealed that the robot was capable of retrieving specimens of masses ranging from 1 gram to 50 grams.

Although RoboCatch was able to successfully demonstrate retrieval of specimens with various sizes, there is still scope for improvements. Some important directions for future work include:

1) Usage of higher-torque motors for the grasping forceps: This would enable RoboCatch to grasp larger and heavier specimens, therefore, enabling more functionality of the device in diverse laparoscopic surgeries.
2) Fabrication of the device using medical grade steel: Although the 3D printing material possessed the biocompatibility criteria, still it could not offer the same rigidity as conventional medical grade alloys. This limitation had a direct impact on the size of the finished product in that we had to scale up the model to make sure that the printed parts possessed an adequate stiffness to undergo the various stresses and forces exerted on it. The current prototype has the outer diameter of 20 mm, which is 5 mm larger than the largest-sized conventional trocars. Fabricating the device out of medical grade steel enables us to scale down the model to a practical size that can be used in conjunction with the conventional laparoscopic trocars.
3) Using a grasping forceps with bigger jaws: The current grasping forceps that is used have medium-sized jaws that makes them good for grasping small to medium-sized specimens. However, to increase the functionality of the grasping forceps, use of a forceps with bigger jaws is a logical step.
4) Increasing the volume of the grasper: The volume of the grasper can be increased in different ways. One is using larger fingers for the grasper. The will enable a bigger volume for containment of larger specimens. Second, use of stronger torsion springs. The torsion spring that were used in the original prototype could not fully lift the distal

and middle links of the webbed grasper due to lack of sufficient torque. Using torsion springs with higher rates can help with the opening of the webbed grasper fully, thus, enabling grasping of larger specimens.

5) Embedding force sensors on the forceps jaws to obtain force feedback while grasping: Force sensors can provide the sensor with essential feedback of the amount of force that the grasper applies on the specimen and would give the surgeon the ability to control the amount of force excreted on the specimen.
6) Design of a better attachment mechanism for the specimen bag: The current specimen bag is permanently attached to the fingers of the grasper. However, with better design considerations simple attachment mechanisms could be developed for disposing of specimen bags after each use and replacing them with new bags.
7) Improving the sealing of the specimen bag after closure: The current system offers containment of the specimen, however it fails to fully seal the bag from leaking of fluids. Designing better mechanisms for the specimen bag closure could solve this problem. One simple solution would be to use soft plastic attachments at the tip of the distal links so that they would seal the bag when the grasper fingers pressed against each other.

With these future extensions to the current design, this research is expected to contribute significantly to the field of minimally invasive surgery by offering an efficient alternative to the existing procedures of specimen retrieval.

REFERENCES

[1] Beard, R. E., & Tsung, A. (2017). Minimally Invasive Approaches for Surgical Management of Primary Liver Cancers, *Cancer Control.* Vol. 24(3), pp. 1-6.

[2] Smita Sihag, Andrzej S. Kosinski, Henning A. Gaissert, Cameron D. Wright, Paul H. Schipper, Minimally Invasive Versus Open Esophagectomy for Esophageal Cancer: A Comparison of Early Surgical Outcomes From The Society of Thoracic Surgeons National Database, *The Annals of Thoracic Surgery*, Vol. 01(4), 2016, pp. 1281-1289.

[3] Raj, P. K., Katris, F., Linderman, C. G., & ReMine, S. G. (1998). An inexpensive laparoscopic specimen retrieval bag. *Surgical endoscopy*, *12*(1), 83-83.

[4] Natalin, R. A., Lima, F. S., Pinheiro, T., Vicari, E., Ortiz, V., Andreoni, C., & Landman, J. (2012). The final stage of the laparoscopic procedure: exploring final steps. *International braz j urol*, *38*(1), 04-16.

[5] Ganpule, A. P., Gotov, E., Mishra, S., Muthu, V., Sabnis, R., & Desai, M. (2010). Novel cost-effective specimen retrieval bag in laparoscopy: Nadiad bag. Urology, 75(5), 1213-1216.

[6] Marcus, H. J., Seneci, C. A., Hughes-Hallett, A., Cundy, T. P., Nandi, D., Yang, G. Z., & Darzi, A. (2016). Comparative performance in single-port versus multiport minimally invasive surgery, and small versus large operative working spaces: a preclinical randomized crossover trial. *Surgical innovation*, *23*(2), 148-155.

[7] Hoeckelmann, M., Rudas, I. J., Fiorini, P., Kirchner, F., & Haidegger, T. (2015). Current Capabilities and Development Potential in Surgical Robotics. International Journal of Advanced Robotic Systems.

[8] Jones, S. (2001). Surgical Aspects and Future Developments of Laparoscopy. Anesthesiology Clinics of North America, 19(1), 107-124.

[9] Üneri, A., Balicki, M. A., Handa, J., Gehlbach, P., Taylor, R. H., & Iordachita, I. (2010, September). New steady-hand eye robot with micro-force sensing for vitreoretinal surgery. In *Biomedical Robotics and Biomechatronics (BioRob), 2010 3rd IEEE RAS and EMBS International Conference on* (pp. 814-819). IEEE.

[10] Jakopec, M., Harris, S. J., y Baena, F. R., Gomes, P., Cobb, J., & Davies, B. L. (2002, September). Preliminary results of an early clinical experience with the Acrobot™ System for total knee replacement surgery. In *International Conference on Medical Image Computing and Computer-Assisted Intervention* (pp. 256-263). Springer, Berlin, Heidelberg.

[11] Payne, C. J., & Yang, G. Z. (2014). Hand-held medical robots. *Annals of biomedical engineering*, *42*(8), 1594-1605.

[12] Mack MJ. Minimally Invasive and Robotic Surgery. *JAMA.* 2001;285(5):568–572. doi:10.1001/jama.285.5.568.

[13] Marcus, H. J., Seneci, C. A., Hughes-Hallett, A., Cundy, T. P., Nandi, D., Yang, G. Z., & Darzi, A. (2016). Comparative performance in single-port versus multiport minimally invasive surgery, and small versus large operative working spaces: a preclinical randomized crossover trial. *Surgical innovation*, *23*(2), 148-155.

[14] Harrell, A. G., & Heniford, B. T. (2005). Minimally invasive abdominal surgery: lux et veritas past, present, and future. *The American journal of surgery*, *190*(2), 239-243.

[15] Camarillo, D. B., Krummel, T. M., & Salisbury Jr, J. K. (2004). Robotic technology in surgery: past, present, and future. *The American Journal of Surgery*, *188*(4), 2-15.

[16] Sanz, C. M., Aguilar, J. F. N., Bogajo, M. L. H., Rivas, A. M., Llorente, C. G., Ruiz, G. T., ... & Yeste, J. S. P. (2010). Single incision laparoscopic surgery. *Cirugía Española (English Edition)*, *88*(1), 12-17.

[17] Dogangil, G., Davies, B. L., & Rodriguez y Baena, F. (2010). A review of medical robotics for minimally invasive soft tissue surgery. *Proceedings of the Institution of Mechanical Engineers, Part H: Journal of Engineering in Medicine*, *224*(5), 653-679.

[18] Ghezzi, F., Cromi, A., Uccella, S., Siesto, G., Bergamini, V., & Bolis, P. (2008). Transumbilical surgical specimen retrieval: a viable refinement of laparoscopic surgery for pelvic masses. *BJOG: An International Journal of Obstetrics & Gynaecology*, *115*(10), 1316-1320.

[19] Stavroulis, A., Memtsa, M., & Yoong, W. (2013). Methods for specimen removal from the peritoneal cavity after laparoscopic excision. *The Obstetrician & Gynaecologist*, *15*(1), 26-30.

[20] Memon, M. A., Deeik, R. K., Maffi, T. R., & Fitzgibbons Jr, R. J. (1999). The outcome of unretrieved gallstones in the peritoneal cavity during laparoscopic cholecystectomy. *Surgical endoscopy*, *13*(9), 848-857.

[21] Mayer, C., Miller, D. M., & Ehlen, T. G. (2002). Peritoneal implantation of squamous cell carcinoma following rupture of a dermoid cyst during laparoscopic removal. *Gynecologic oncology*, *84*(1), 180-183.

[22] Chou, L. Y., Sheu, B. C., Chang, D. Y., Huang, S. C., Chen, S. Y., Hsu, W. C., & Chang, W. C. (2010). Comparison between transumbilical and transabdominal ports for the laparoscopic

retrieval of benign adnexal masses: a randomized trial. *European Journal of Obstetrics & Gynecology and Reproductive Biology*, *153*(2), 198-202.

[23] Edwards, M. (1984). Robots in industry: An overview. *Applied ergonomics*, *15*(1), 45-53.

[24] Heyer, C. (2010, October). Human-robot interaction and future industrial robotics applications. In *Intelligent Robots and Systems (IROS), 2010 IEEE/RSJ International Conference on*(pp. 4749-4754). IEEE.

[25] A. Suprem,N.Mahalik, and K. Kim, "A reviewon application of technologysystems, standards and interfaces for agriculture and food sector," *Comput. Standards Interfaces*, vol. 35, pp. 355–364, 2013.

[26] G. Hirzinger, "Robots in space—A survey," *Adv. Robot.*, vol. 9, pp. 625–651, 1994.

[27] I. Leite, C. Martinho, and A. Paiva, "Social robots for long-term interaction: A survey," *Int. J. Soc. Robot.*, vol. 5, no. 2, pp. 291–308, 2013.

[28] Burgner-Kahrs, J., Rucker, D. C., & Choset, H. (2015). Continuum robots for medical applications: A survey. *IEEE Transactions on Robotics*, *31*(6), 1261-1280.

[29] Thomas, D., Scholz, E. P., Schweizer, P. A., Katus, H. A., & Becker, R. (2012). Initial experience with robotic navigation for catheter ablation of paroxysmal and persistent atrial fibrillation. *Journal of electrocardiology*, *45*(2), 95-101.

[30] Sackier, J. M., & Wang, Y. (1994). Robotically assisted laparoscopic surgery. *Surgical en*

[31] Schurr MO, Arezzo A, Neisius B, Rininsland H, Hilzinger HU, Dom J et al. Trocar and instrument positioning system TISKA. An assist device for endoscopic solo surgery. Surg Endosc 1999; 13: 528-31.

[32] Buess GF, Arezzo A, Schurr MO, Ulmer F, Fisher H, Gumb L et al. A new remote-controlled endoscope positioning system for endoscopic solo surgery. The FIPS endoarm [see comments]. Surg Endosc 2000; 14:395-9.

[33] Schurr MO, Arezzo A, Buess GE Robotics and systems technology for advanced endoscopic procedures: experiences in general surgery. EurJ Cardiothorac Surg 1999; 16 (Suppl 2): S97-105.

[34] Ruurda, J. P., Van Vroonhoven, T. J., & Broeders, I. A. M. J. (2002). Robot-assisted surgical systems: a new era in laparoscopic surgery. *Annals of the Royal College of Surgeons of England*, *84*(4), 223.

[35] Bowersox JC, Shah A, Jensen J, Bill J, Cordts PR, Green PS. Vascular applications of telepresence surgery: initial feasibility studies in swine. I Vasc Surg 1996; 23:281-7.

[36] Sung, G. T., & Gill, I. S. (2001). Robotic laparoscopic surgery: a comparison of the da Vinci and Zeus systems. *Urology*, *58*(6), 893-898.

[37] Lehman, A. C., Berg, K. A., Dumpert, J., Wood, N. A., Visty, A. Q., Rentschler, M. E., ... & Oleynikov, D. (2008). Surgery with cooperative robots. *Computer Aided Surgery*, *13*(2), 95-105.

[38] Taylor, R., Jensen, P., Whitcomb, L., Barnes, A., Kumar, R., Stoianovici, D., ... & Kavoussi, L. (1999). A steady-hand robotic system for microsurgical augmentation. *The International Journal of Robotics Research*, *18*(12), 1201-1210.

[39] Zahraee, A. H., Paik, J. K., Szewczyk, J., & Morel, G. (2010). Toward the development of a hand-held surgical robot for laparoscopy. *IEEE ASME Transactions on Mechatronics*, *15*(6), 853.

[40] Zhan, Y., Duan, X. G., & Li, J. X. (2015, August). Review of comanipulation robot in surgery. In *Mechatronics and Automation (ICMA), 2015 IEEE International Conference on*(pp. 1466-1471). IEEE.

[41] MacLachlan, R. A., Becker, B. C., Tabarés, J. C., Podnar, G. W., Lobes Jr, L. A., & Riviere, C. N. (2012). Micron: an actively stabilized handheld tool for microsurgery. *IEEE transactions on robotics: a publication of the IEEE Robotics and Automation Society*, *28*(1), 195.

[42] Saxena, A., and R. V. Patel. An active handheld device for compensation of physiological tremor using an ionic polymer metallic composite actuator. In: IEEE/RSJ International Conference on Intelligent Robots and Systems, pp. 4275–4280, 2013.

[43] Song, C., D. Y. Park, P. L. Gehlbach, S. J. Park, and J. U. Kang. Fiber-optic OCT sensor guided ‘‘SMART’’ microforceps for microsurgery. Biomed. Optics. Exp. 4:1045– 1050, 2013.

[44] Isakov, A., Murdaugh, K. M., Burke, W. C., Zimmerman, S., Roche, E., Holland, D., ... & Walsh, C. J. (2014). A new laparoscopic morcellator using an actuated wire mesh and bag. *Journal of Medical Devices*, *8*(1), 011009.

[45] Dario, P., M. C. Carrozza, M. Marcacci, S. D’Attanasio, B. Magnami, O. Tonet, and G. Megali. A novel mechatronic tool for computer-assisted arthroscopy. IEEE Trans. Inf. Technol. Biomed. 4:15–29, 2000.

[46] Gonenc, B., Chamani, A., Handa, J., Gehlbach, P., Taylor, R. H., & Iordachita, I. (2017). 3-dof force-sensing motorized micro-forceps for robot-assisted vitreoretinal surgery. *IEEE sensors journal*, *17*(11), 3526-3541.

[47] Mirbagheri, A., & Farahmand, F. (2013). A triple-jaw actuated and sensorized instrument for grasping large organs during minimally invasive robotic surgery. *The International Journal of Medical Robotics and Computer Assisted Surgery*, *9*(1), 83-93.

[48] Gafford, J., Ding, Y., Harris, A., McKenna, T., Polygerinos, P., Holland, D., ... & Walsh, C. (2014). Shape deposition manufacturing of a soft, atraumatic, deployable surgical grasper. *Journal of Medical Devices*, *8*(3), 030927.

[49] Payne, C. J., Latt, W. T., & Yang, G. Z. (2012, May). A new hand-held force-amplifying device for micromanipulation. In *Robotics and Automation (ICRA), 2012 IEEE International Conference on* (pp. 1583-1588). IEEE.

[50] Yao, H.-Y., V. Hayward, and R. E. Ellis. A tactile enhancement instrument for minimally invasive surgery. Comput. Aided. Surg. 10:233–239, 2005.

[51] Akdemir, A., Ergenoğlu, A. M., Akman, L., Yeniel, A. Ö., Şendağ, F., & Öztekin, M. K. (2013). A novel technique for laparoscopic removal of the fallopian tube after ectopic pregnancy via transabdominal or transumbilical port using homemade bag: A randomized trial. *Journal of research in medical sciences: the official journal of Isfahan University of Medical Sciences*, *18*(9), 777.

[52] Kuo, C. H., Dai, J. S., & Dasgupta, P. (2012). Kinematic design considerations for minimally invasive surgical robots: an overview. *The International Journal of Medical Robotics and Computer Assisted Surgery*, *8*(2), 127-145.

[53] Taylor, R. H., Menciassi, A., Fichtinger, G., Fiorini, P., & Dario, P. (2016). Medical robotics and computer-integrated surgery. In *Springer handbook of robotics* (pp. 1657-1684). Springer, Cham.

[54] Davies, B. L. (1996). A discussion of safety issues for medical robots. *Computer-Integrated Surgery*, 287-296.

[55] Kajbafzadeh, A. M., Javan-Farazmand, N., Monajemzadeh, M., & Baghayee, A. (2013). Determining the optimal decellularization and sterilization protocol for preparing a tissue scaffold of a human-sized liver tissue. *Tissue Engineering Part C: Methods*, *19*(8), 642-651.

[56] Berguer, R. (1999). Surgery and ergonomics. *Archives of surgery*, *134*(9), 1011-1016.

[57] Kaya, O. I., Moran, M., Ozkardes, A. B., Taskin, E. Y., Seker, G. E., & Ozmen, M. M. (2008). Ergonomic problems encountered by the surgical team during video endoscopic surgery. *Surgical Laparoscopy Endoscopy & Percutaneous Techniques*, *18*(1), 40-44.

[58] Wang, C. Y., & Cai, D. C. (2017). Hand tool handle design based on hand measurements. In *MATEC Web of Conferences* (Vol. 119, p. 01044). EDP Sciences.

[59] Lanfranco, A. R., Castellanos, A. E., Desai, J. P., & Meyers, W. C. (2004). Robotic surgery: a current perspective. *Annals of surgery*, *239*(1), 14.

[60] https://wlsurgeries.weebly.com/laparoscopic-vs-open-procedures.html

[61] https://www.reichelt.com/de/en/usb-2-0-endoscope-camera-8-mm-endo-kam-usb2-p89624.html

[62] http://www.continentalhospitals.com/blog/minimally-invasive-surgery-for-cancer-the-best-alternative-to-open-surgery/#prettyPhoto

[63] https://drheidarizadi.com/learning-center/single-port-surgery.html

[64] https://www.shutterstock.com/video/clip-1900282-heart-beats-through-open-chest-during-surgery

[65] https://www.theexpertinstitute.com/complications-laparoscopic-robotic-surgery/

[66] Jategaonkar, Priyadarshan & Pradeep Yadav, Sudeep. (2013). Trans-umbilical Laparoscopic Appendectomy for Acute Appendicitis without Raising Skin-flaps: An Easy-to-use Modification

Applied to the Series of 164 Patients from a Rural Institute of Central India. Journal of surgical technique and case report. 5. 8-12. 10.4103/2006-8808.118593.

[67] https://www.imperial.ac.uk/people/p.korzeniowski/research.html

[68] https://www.medtronic.com/covidien/en-us/products/hand-instruments-ligation/specimen-retrieval-products.html

[69] https://www.youtube.com/watch?v=54TJjs4HcbU

[70] https://www.youtube.com/watch?v=WvobSjGCPE4

[71] https://www.chandanhospital.in/general-laparoscopic-surgery.aspx

[72] https://www.fool.com/investing/2018/01/16/heres-how-intuitive-surgical-inc-crushed-it-in-201.aspx

VITA

Farid Tavakkolmoghaddam

Mechanical & Aerospace Engineering
Old Dominion University
115 Kaufman Hall, Norfolk, VA 23529

EDUCATION

Master of Science in Mechanical Engineering at Old Dominion University, December 2018, Thesis title: "ROBOCATCH: DESIGN AND MAKING OF A HAND-HELD SPILLAGE-FREE SPECIMEN RETRIEVAL ROBOT FOR LAPAROSCOPIC SURGERY"

Bachelor of Science in Mechanical Engineering at Islamic Azad University, September 2015

ACADEMIC EMPLOYMENT

Graduate Teaching Assistant for MAE 225 Solid Mechanics Lab to Dr. Ramamurthy Prabhakaran, Department of Mechanical & Aerospace Engineering, Old Dominion University, May 2017 – December 2018. Responsibilities included Planning, preparation, and instruction of the assigned curriculum. Demonstrated the experiments and software to students. Provided support and guidance to students, evaluated students' lab reports and exams. Maintained records of students' grades.

Graduate Teaching Assistant for MAE 312 Thermodynamics II to Dr. Sushil Chaturvedi, Department of Mechanical & Aerospace Engineering, Old Dominion University, Jan 2017 – May 2017. Responsibilities included grading homework, projects, and exams.

Graduate Teaching Assistant for MAE 495 Solid Mechanics Lab to Dr. Arthur Taylor, Department of Mechanical & Aerospace Engineering, Old Dominion University, Jan 2017 – May 2017. Responsibilities included grading homework, projects, and exams.